Uang, C., Tsai, K., Bruneau, M. "Seismic Design of Steel Bridges."
Bridge Engineering Handbook.
Ed. Wai-Fah Chen and Lian Duan
Boca Raton: CRC Press, 2000

39

Seismic Design of Steel Bridges

Chia-Ming Uang
University of California, San Diego

Keh-Chyuan Tsai
National Taiwan University

Michel Bruneau
State University of New York, Buffalo

39.1   Introduction

In the aftermath of the 1995 Hyogo-ken Nanbu earthquake and the extensive damage it imparted
to steel bridges in the Kobe area, it is now generally recognized that steel bridges can be seismically
vulnerable, particularly when they are supported on nonductile substructures of reinforced concrete,
masonry, or even steel. In the last case, unfortunately, code requirements and guidelines on seismic
design of ductile bridge steel substructures are few [12,21], and none have yet been implemented
in the United States. This chapter focuses on a presentation of concepts and detailing requirements
that can help ensure a desirable ductile behavior for steel substructures. Other bridge vulnerabilities
common to all types of bridges, such as bearing failure, span collapses due to insufficient seat width
or absence of seismic restrainers, soil liquefactions, etc., are not addressed in this chapter.

39.1.1   Seismic Performance Criteria

The American Association of State Highway and Transportation Officials (AASHTO) published
both the *Standard Specifications for Highway Bridges* [2] and the *LRFD Bridge Design Specifications*
[1], the latter being a load and resistance factor design version of the former, and being the preferred
edition when referenced in this chapter. Although notable differences exist between the seismic

design requirements of these documents, both state that the same fundamental principles have been used for the development of their specifications, namely:

1. Small to moderate earthquakes should be resisted within the elastic range of the structural components without significant damage.
2. Realistic seismic ground motion intensities and forces are used in the design procedures.
3. Exposure to shaking from large earthquakes should not cause collapse of all or part of the bridge. Where possible, damage that does occur should be readily detectable and accessible for inspection and repair.

Conceptually, the above performance criteria call for two levels of design earthquake ground motion to be considered. For a low-level earthquake, there should be only minimal damage. For a significant earthquake, which is defined by AASHTO as having a 10% probability of exceedance in 50 years (i.e., a 475-year return period), collapse should be prevented but significant damage may occur. Currently, the AASHTO adopts a simplified approach by specifying only the second-level design earthquake; that is, the seismic performance in the lower-level events can only be implied from the design requirements of the upper-level event. Within the content of performance-based engineering, such a one-level design procedure has been challenged [11,12].

The AASHTO also defines bridge importance categories, whereby essential bridges and critical bridges are, respectively, defined as those that must, at a minimum, remain open to emergency vehicles (and for security/defense purposes), and be open to all traffic, after the 475-year return-period earthquake. In the latter case, the AASHTO suggests that critical bridges should also remain open to emergency traffic after the 2500-year return-period event. Various clauses in the specifications contribute to ensure that these performance criteria are implicitly met, although these may require the engineer to exercise considerable judgment. The special requirements imposed on essential and critical bridges are beyond the scope of this chapter.

39.1.2   The *R* Factor Design Procedure

AASHTO seismic specification uses a response modification factor, *R*, to compute the design seismic forces in different parts of the bridge structure. The origin of the *R* factor design procedure can be traced back to the ATC 3-06 document [9] for building design. Since requirements in seismic provisions for member design are directly related to the *R* factor, it is worthwhile to examine the physical meaning of the *R* factor.

Consider a structural response envelope shown in Figure 39.1. If the structure is designed to respond elastically during a major earthquake, the required elastic force, Q_e, would be high. For economic reasons, modern seismic design codes usually take advantage of the inherent energy dissipation capacity of the structure by specifying a design seismic force level, Q_s, which can be significantly lower than Q_e:

$$Q_s = \frac{Q_e}{R} \tag{39.1}$$

The energy dissipation (or ductility) capacity is achieved by specifying stringent detailing requirements for structural components that are expected to yield during a major earthquake. The design seismic force level Q_s is the first significant yield level of the structure, which corresponds to the level beyond which the structural response starts to deviate significantly from the elastic response. Idealizing the actual response envelope by a linearly elastic–perfectly plastic response shown in Figure 39.1, it can be shown that the *R* factor is composed of two contributing factors [64]:
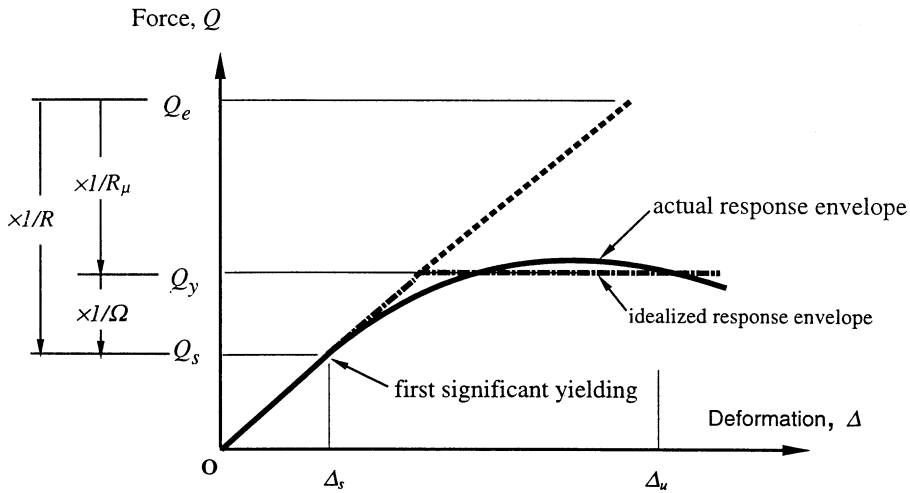
$$R = R_\mu \Omega \tag{39.2}$$

FIGURE 39.1   Concept of response modification factor, *R*.

TABLE 39.1   Response Modification Factor, *R*

Substructure	R	Connections	R
Single columns	3	Superstructure to abutment	0.8
Steel or composite steel and concrete pile bents		Columns, piers, or pile bents to cap beam or superstructure	1.0
a. Vertical piles only	5		
b. One or more batter piles	3		1.0
Multiple column bent	5	Columns or piers to foundations	

Source: AASHTO, *Standard Specifications for Seismic Design of Highway Bridges*, AASHTO, Washington, D.C., 1992.

The ductility reduction factor, R_μ, accounts for the reduction of the seismic force level from Q_e to Q_y. Such a force reduction is possible because ductility, which is measured by the ductility factor $\mu \Delta_u / \Delta_y$), is built into the structural system. For single-degree-of-freedom systems, relationships between μ and R_μ have been proposed (e.g., Newmark and Hall [43]).

The structural overstrength factor, Ω, in Eq. (39.2) accounts for the reserve strength between the seismic resistance levels Q_y and Q_s. This reserve strength is contributed mainly by the redundancy of the structure. That is, once the first plastic hinge is formed at the force level Q_s, the redundancy of the structure would allow more plastic hinges to form in other designated locations before the ultimate strength, Q_y, is reached. Table 39.1 shows the values of *R* assigned to different substructure and connection types. The AASHTO assumes that cyclic inelastic action would only occur in the substructure; therefore, no *R* value is assigned to the superstructure and its components. The table shows that the *R* value ranges from 3 to 5 for steel substructures. A multiple column bent with well detailed columns has the highest value (= 5) of *R* due to its ductility capacity and redundancy. The ductility capacity of single columns is similar to that of columns in multiple column bent; however, there is no redundancy and, therefore, a low *R* value of 3 is assigned to single columns.

Although modern seismic codes for building and bridge designs both use the *R* factor design procedure, there is one major difference. For building design [42], the *R* factor is applied at the system level. That is, components designated to yield during a major earthquake share the same *R* value, and other components are proportioned by the capacity design procedure to ensure that these components remain in the elastic range. For bridge design, however, the *R* factor is applied at the component level. Therefore, different *R* values are used in different parts of the same structure.
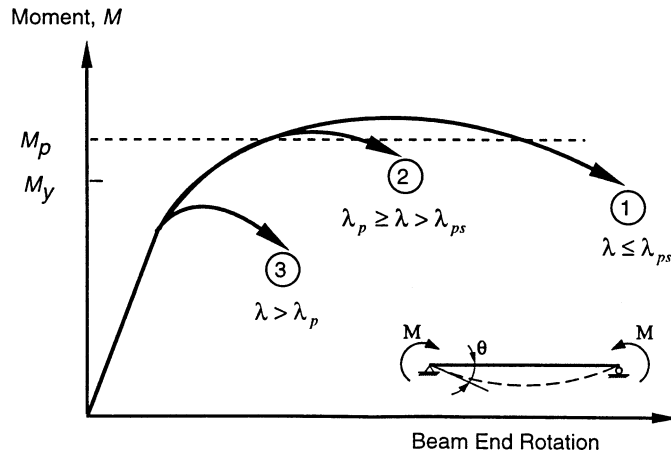
FIGURE 39.2 Effect of beam slenderness ratio on strength and deformation capacity. (Adapted from Yura et al., 1978.)

39.1.3 Need for Ductility

Using an R factor larger than 1 implies that the ductility demand must be met by designing the structural component with stringent requirements. The ductility capacity of a steel member is generally governed by instability. Considering a flexural member, for example, instability can be caused by one or more of the following three limit states: flange local buckling, web local buckling, and lateral-torsional buckling. In all cases, ductility capacity is a function of a slenderness ratio, λ. For local buckling, λ is the width–thickness ratio; for lateral-torsional buckling, λ is computed as L_b/r_y, where L_b is the unbraced length and r_y is the radius of gyration of the section about the buckling axis. Figure 39.2 shows the effect of λ on strength and deformation capacity of a wide-flanged beam. Curve 3 represents the response of a beam with a noncompact or slender section; both its strength and deformation capacity are inadequate for seismic design. Curve 2 corresponds to a beam with "compact" section; its slenderness ratio, λ, is less than the maximum ratio λp for which a section can reach its plastic moment, M_p, and sustain moderate plastic rotations. For seismic design, a response represented by Curve 1 is needed, and a "plastic" section with λ less than λps is required to deliver the needed ductility.

Table 39.2 shows the limiting width–thickness ratios λp and λps for compact and plastic sections, respectively. A flexural member with λ not exceeding λp can provide a rotational ductility factor of at least 4 [74], and a flexural member with λ less than λps is expected to deliver a rotation ductility factor of 8 to 10 under monotonic loading [5]. Limiting slenderness ratios for lateral-torsional buckling are presented in Section 39.2.

39.1.4 Structural Steel Materials

AASHTO M270 (equivalent to ASTM A709) includes grades with a minimum yield strength ranging from 36 to 100 ksi (see Table 39.3). These steels meet the AASHTO Standards for the mandatory notch toughness and weldability requirements and hence are prequalified for use in welded bridges.

For ductile substructure elements, steels must be capable of dissipating hysteretic energy during earthquakes, even at low temperatures if such service conditions are expected. Typically, steels that have $F_y < 0.8F_u$ and can develop a longitudinal elongation of 0.2 mm/mm in a 50-mm gauge length prior to failure at the expected service temperature are satisfactory.

TABLE 39.2 Limiting Width-Thickness Ratios

Description of Element	Width-Thickness Ratio	λ_p	λ_{ps}
Flanges of I-shaped rolled beams, hybrid or welded beams, and channels in flexure	b/t	$65/(\sqrt{F_y})$	$52/(\sqrt{F_y})$
Webs in combined flexural and axial compression	h/t_w	for $P_u/\phi bPy \leq 0.125$: $$\frac{640}{\sqrt{F_y}}\left(1-\frac{2.75P_u}{\phi_b P_y}\right)$$ for $P_u/\phi_b P_y > 0.125$: $$\frac{191}{\sqrt{F_y}}\left(2.33-\frac{P_u}{\phi_b P_y}\right) \geq \frac{253}{\sqrt{F_y}}$$	for $Pu/\phi bPy > 0.125$: $$\frac{520}{\sqrt{F_y}}\left(1-\frac{1.54P_u}{\phi_b P_y}\right)$$ for $P_u/\phi_b P_y > 0.125$: $$\frac{191}{\sqrt{F_y}}\left(2.33-\frac{P_u}{\phi_b P_y}\right) \geq \frac{253}{\sqrt{F_y}}$$
Round HSS in axial compression or flexure	D/t	$\dfrac{2070}{F_y}$	$\dfrac{1300}{F_y}$
Rectangular HSS in axial compression or flexure	b/t	$\dfrac{190}{\sqrt{F_y}}$	$\dfrac{110}{\sqrt{F_y}}$

Note: F_y in ksi, $\phi_b = 0.9$.

Source: AISC, *Seismic Provisions for Structural Steel Buildings*, AISC, Chicago, IL, 1997.

TABLE 39.3 Minimum Mechanical Properties of Structural Steel

AASHTO Designation	M270 Grade 36	M270 Grade 50	M270 Grade 50W	M270 Grade 70W	M270 Grades 100/100W	
Equivalent ASTM designation	A709 Grade 36	A709 Grade 50	A709 Grade 50W	A709 Grade 70W	A709 Grade 100/100W	
Minimum yield stress (ksi)	36	50	50	70	100	90
Minimum tensile stress (ksi)	58	65	70	90	110	100

Source: AASHTO, *Standard Specification for Highway Bridges*, AASHTO, Washington, D.C., 1996.

39.1.5 Capacity Design and Expected Yield Strength

For design purposes, the designer is usually required to use the minimum specified yield and tensile strengths to size structural components. This approach is generally conservative for gravity load design. However, this is not adequate for seismic design because the AASHTO design procedure sometimes limits the maximum force acting in a component to the value obtained from the adjacent yielding element, per a capacity design philosophy. For example, steel columns in a multiple-column bent can be designed for an *R* value of 5, with plastic hinges developing at the column ends. Based on the weak column–strong beam design concept (to be presented in Section 39.2), the cap beam and its connection to columns need to be designed elastically (i.e., *R* = 1, see Table 39.1). Alternatively, for bridges classified as seismic performance categories (SPC) C and D, the AASHTO recommends that, for economic reasons, the connections and cap beam be designed for the maximum forces capable of being developed by plastic hinging of the column or column bent; these forces will often be significantly less than those obtained using an *R* factor of 1. For that purpose, recognizing the possible overstrength from higher yield strength and strain hardening, the AASHTO [1] requires that the column plastic moment be calculated using 1.25 times the nominal yield strength.

Unfortunately, the widespread brittle fracture of welded moment connections in steel buildings observed after the 1994 Northridge earthquake revealed that the capacity design procedure mentioned

TABLE 39.4 Expected Steel Material Strengths (SSPC 1994)

Steel Grade	A36	A572 Grade 50
No. of Sample	36,570	13,536
Yield Strength (COV)	49.2 ksi (0.10)	57.6 ksi (0.09)
Tensile Strength (COV)	68.5 ksi (0.07)	75.6 ksi (0.08)

COV: coefficient of variance.

Source: SSPC, *Statistical Analysis of Tensile Data for Wide Flange Structural Shapes,* Structural Shapes Producers Council, Washington, D.C., 1994.

above is flawed. Investigations that were conducted after the 1994 Northridge earthquake indicate that, among other factors, material overstrength (i.e., the actual yield strength of steel is significantly higher than the nominal yield strength) is one of the major contributing factors for the observed fractures [52].

Statistical data on material strength of AASHTO M270 steels is not available, but since the mechanical characteristics of M270 Grades 36 and 50 steels are similar to those of ASTM A36 and A572 Grade 50 steels, respectively, it is worthwhile to examine the expected yield strength of the latter. Results from a recent survey [59] of certified mill test reports provided by six major steel mills for 12 consecutive months around 1992 are briefly summarized in Table 39.4. Average yield strengths are shown to greatly exceed the specified values. As a result, relevant seismic provisions for building design have been revised. The AISC Seismic Provisions [6] use the following formula to compute the expected yield strength, *Fye*, of a member that is expected to yield during a major earthquake:

$$F_{ye} = R_y F_y \qquad (39.3)$$

where *Fy* is the specified minimum yield strength of the steel. For rolled shapes and bars, R_y should be taken as 1.5 for A36 steel and 1.1 for A572 Grade 50 steel. When capacity design is used to calculate the maximum force to be resisted by members connected to yielding members, it is suggested that the above procedure also be used for bridge design.

39.1.6 Member Cyclic Response

A typical cyclic stress–strain relationship of structural steel material is shown in Figure 39.3. When instability are excluded, the figure shows that steel is very ductile and is well suited for seismic applications. Once the steel is yielded in one loading direction, the Bauschinger effect causes the steel to yield earlier in the reverse direction, and the clearly defined yield plateau disappears in subsequent cycles. Where instability needs to be considered, the Bauschinger effect may affect the cyclic strength of a steel member.

Consider an axially loaded steel member first. Figure 39.4 shows the typical cyclic response of an axially loaded tubular brace. The initial buckling capacity can be predicted reliably using the tangent modulus concept [47]. The buckling capacity in subsequent cycles, however, is reduced due to two factors: (1) the Bauschinger effect, which reduces the tangent modulus, and (2) the increased out-of-straigthness as a result of buckling in previous cycles. Such a reduction in cyclic buckling strength needs to be considered in design (see Section 39.3).

For flexural members, repeated cyclic loading will also trigger buckling even though the width–thickness ratios are less than the λps limits specified in Table 39.2. Figure 39.5 compares the cyclic response of two flexural members with different flange *b/t* ratios [62]. The strength of the beam having a larger flange width–thickness ratio degrades faster under cyclic loading as local buckling develops. This justifies the need for more stringent slenderness requirements in seismic design than those permitted for plastic design.
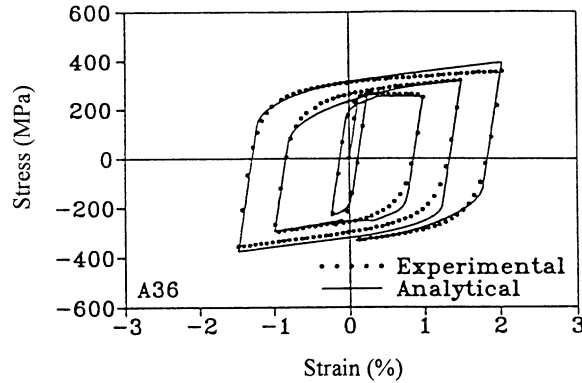
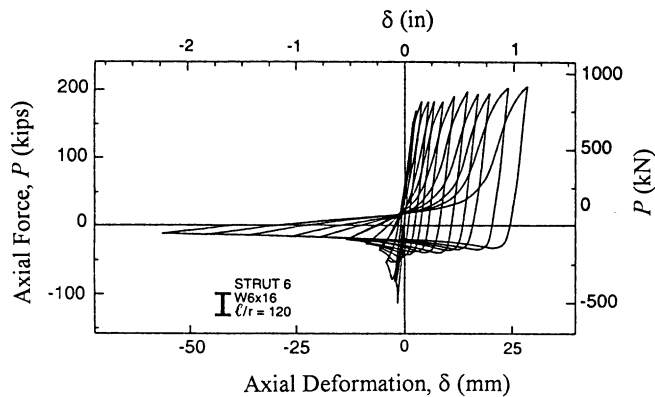**FIGURE 39.3** Typical cyclic stress–strain relationship of structural steel.


FIGURE 39.4 Cyclic response of an axially loaded member. (Source: Popov, E. P. and Black, W., *J. Struct. Div. ASCE*, 90(ST2), 223-256, 1981. With permission.)

## 39.2 Ductile Moment-Resisting Frame (MRF) Design

39.2.1 Introduction

The prevailing philosophy in the seismic resistant design of ductile frames in buildings is to force plastic hinging to occur in beams rather than in columns in order to better distribute hysteretic energy throughout all stories and to avoid soft-story-type failure mechanisms. However, for steel bridges such a constraint is not realistic, nor is it generally desirable. Steel bridges frequently have deep beams which are not typically compact sections, and which are much stiffer flexurally than their supporting steel columns. Moreover, bridge structures in North America are generally "single-story" (single-tier) structures, and all the hysteretic energy dissipation is concentrated in this single story. The AASHTO [3] and CHBDC [21] seismic provisions are, therefore, written assuming that columns will be the ductile substructure elements in moment frames and bents. Only the CHBDC, to date, recognizes the need for ductile detailing of steel substructures to ensure that the performance objectives are met when an *R* value of 5 is used in design [21]. It is understood that extra care would be needed to ensure the satisfactory ductile response of multilevel steel frame bents since these are implicitly not addressed by these specifications. Note that other recent design recommendations [12] suggest that the designer can choose to have the primary energy dissipation mechanism occur in either the beam–column panel zone or the column, but this approach has not been implemented in codes.
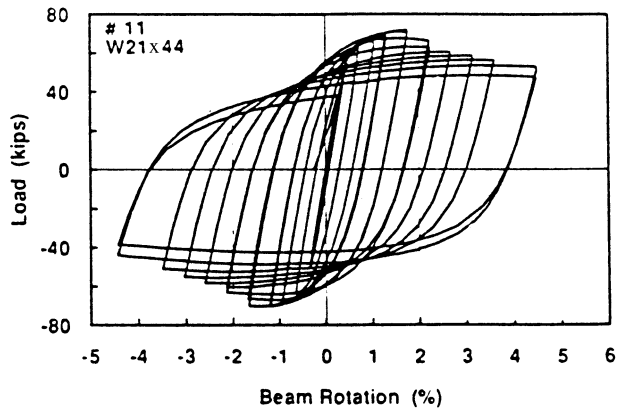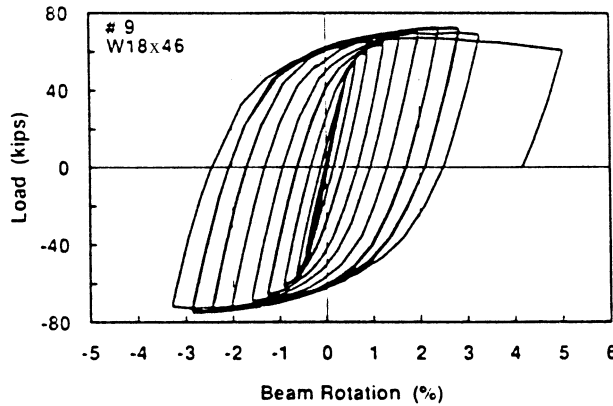
FIGURE 39.5 Effect of beam flange width–thickness ratio on strength degradation. (a) $b_f/2t_f$ = 7.2; (b) $b_f/2t_f$= 5.0.

Some detailing requirements are been developed for elements where inelastic deformations are expected to occur during an earthquake. Nevertheless, lessons learned from the recent Northridge and Hyogo-ken Nanbu earthquakes have indicated that steel properties, welding electrodes, and connection details, among other factors, all have significant effects on the ductility capacity of welded steel beam–column moment connections [52]. In the case where the bridge column is continuous and the beam is welded to the column flange, the problem is believed to be less severe as the beam is stronger and the plastic hinge will form in the column [21]. However, if the bridge girder is continuously framed over the column in a single-story frame bent, special care would be needed for the welded column-to-beam connections.

Continuous research and professional developments on many aspects of the welded moment connection problems are well in progress and have already led to many conclusions that have been implemented on an interim basis for building constructions [52,54]. Many of these findings should be applicable to bridge column-to-beam connections where large inelastic demands are likely to
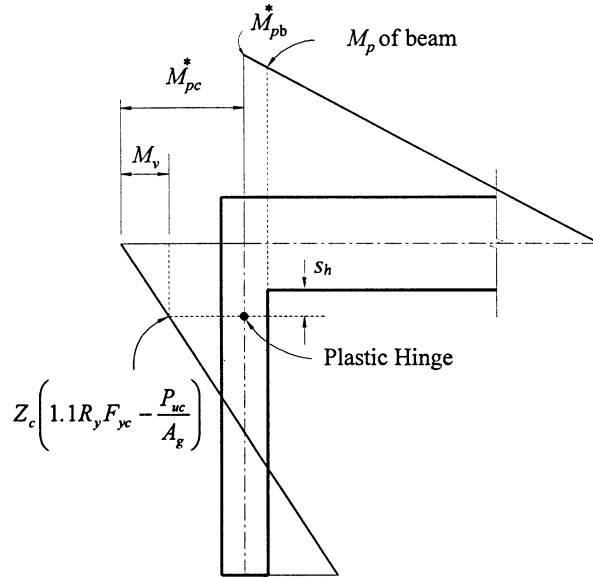
FIGURE 39.6   Location of plastic hinge.

develop in a major earthquake. The following sections provide guidelines for the seismic design of steel moment-resisting beam–column bents.

39.2.2   Design Strengths

Columns, beams, and panel zones are first designed to resist the forces resulting from the prescribed load combinations; then capacity design is exercised to ensure that inelastic deformations only occur in the specially detailed ductile substructure elements. To ensure a weak-column and strong-girder design, the beam-to-column strength ratio must satisfy the following requirement:

$$\frac{\sum M_{pb}^*}{\sum M_{pc}^*} \geq 1.0 \tag{39.4}$$

where $\sum M_{pb}^*$ is the sum of the beam moments at the intersection of the beam and column centerline. It can be determined by summing the projections of the nominal flexural strengths, M_p ($= Z_b F_y$, where Z_b is the plastic section modulus of the beam), of the beams framing into the connection to the column centerline. The term $\sum M_{pc}^*$ is the sum of the expected column flexural strengths, reduced to account for the presence of axial force, above and below the connection to the beam centerlines. The term $\sum M_{pc}^*$ can be approximated as $\sum [Z_c(1.1 R_y F_{yc} - P_{uc}/A_g) + M_v]$, where A_g is the gross area of the column, P_{uc} is the required column compressive strength, Z_c is the plastic section modulus of the column, F_{yc} is the minimum specified yield strength of the column. The term M_v is to account for the additional moment due to shear amplification from the actual location of the column plastic hinge to the beam centerline (Figure 39.6). The location of the plastic hinge is at a distance s_h from the edge of the reinforced connection. The value of s_h ranges from one quarter to one third of the column depth as suggested by SAC [54].

To achieve the desired energy dissipation mechanism, it is rational to incorporate the expected yield strength into recent design recommendations [12,21]. Furthermore, it is recommended that the beam–column connection and the panel zone be designed for 125% of the expected plastic

bending moment capacity, $Z_c(1.1R_yF_{yc} - P_{uc}/A_g)$, of the column. The shear strength of the panel zone, V_n, is given by

$$V_n = 0.6F_y d_c t_p \qquad (39.5)$$

where d_c is the overall column depth and t_p is the total thickness of the panel zone including doubler plates. In order to prevent premature local buckling due to shear deformations, the panel zone thickness, t_p, should conform to the following:

$$t_p \geq \frac{d_z + w_z}{90} \qquad (39.6)$$

where d_z and w_z are the panel zone depth and width, respectively.

Although weak panel zone is permitted by the AISC [6] for building design, the authors, however, prefer a conservative approach in which the primary energy dissipation mechanism is column hinging.

39.2.3 Member Stability Considerations

The width–thickness ratios of the stiffened and unstiffened elements of the column section must not be greater than the λ_{ps} limits given in Table 39.2 in order to ensure ductile response for the plastic hinge formation. Canadian practice [21] requires that the factored axial compression force due to the seismic load and gravity loads be less than $0.30A_gF_y$ (or twice that value in lower seismic zones). In addition, the plastic hinge locations, near the top and base of each column, also need to be laterally supported. To avoid lateral-torsional buckling, the unbraced length should not exceed $2500r_y/F_y$ [6].

39.2.4 Column-to-Beam Connections

Widespread brittle fractures of welded moment connections in building moment frames that were observed following the 1994 Northridge earthquake have raised great concerns. Many experimental and analytical studies conducted after the Northridge earthquake have revealed that the problem is not a simple one, and no single factor can be made fully responsible for the connection failures. Several design advisories and interim guidelines have already been published to assist engineers in addressing this problem [52,54]. Possible causes for the connection failures are presented below.

1. As noted in Section 39.1.5, the mean yield strength of A36 steel in the United States is substantially higher than the nominal yield value. This increase in yield strength combined with the cyclic strain hardening effect can result in a beam moment significantly higher than its nominal strength. Considering the large variations in material strength, it is questionable whether the bolted web-welded flange pre-Northridge connection details can reliably sustain the beam flexural demand imposed by a severe earthquake.

2. Recent investigations conducted on the properties of weld metal have indicated that the E70T-4 weld metal which was typically used in many of the damaged buildings possesses low notch toughness [60]. Experimental testing of welded steel moment connections that were conducted after the Northridge earthquake clearly demonstrated that notch-tough electrodes are needed for seismic applications. Note that the bridge specifications effectively prohibit the use of E70T-4 electrode.

3. In a large number of connections, steel backing below the beam bottom flange groove weld has not been removed. Many of the defects found in such connections were slag inclusions of a size that should have been rejected per AWS D1.1 if they could have been detected during

the construction. The inclusions were particularly large in the middle of the flange width where the weld had to be interrupted due to the presence of the beam web. Ultrasonic testing for welds behind the steel backing and particularly near the beam web region is also not very reliable. Slag inclusions are equivalent to initial cracks, which are prone to crack initiation at a low stress level. For this reason, the current steel building welding code [13] requires that steel backing of groove welds in cyclically loaded joints be removed. Note that the bridge welding code [14] has required the removal of steel backing on welds subjected to transverse tensile stresses.

4. Steel that is prevented from expanding or contracting under stress can fail in a brittle manner. For the most common type of groove welded flange connections used prior to the Northridge earthquake, particularly when they were executed on large structural shapes, the welds were highly restrained along the length and in the transverse directions. This precludes the welded joint from yielding, and thus promotes brittle fractures [16].

5. Rolled structural shapes or plates are not isotropic. Steel is most ductile in the direction of rolling and least ductile in the direction orthogonal to the surface of the plate elements (i.e., through-thickness direction). Thicker steel shapes and plates are also susceptible to lamellar tearing [4].

After the Northridge earthquake, many alternatives have been proposed for building construction and several have been tested and found effective to sustain cyclic plastic rotational demand in excess of 0.03 rad. The general concept of these alternatives is to move the plastic hinge region into the beam and away from the connection. This can be achieved by either strengthening the beam near the connection or reducing the strength of the yielding member near the connection. The objective of both schemes is to reduce the stresses in the flange welds in order to allow the yielding member to develop large plastic rotations. The minimum strength requirement for the connection can be computed by considering the expected maximum bending moment at the plastic hinge using statics similar to that outlined in Section 39.2.2. Capacity-enhancement schemes which have been widely advocated include cover plate connections [26] and bottom haunch connections. The demand-reduction scheme can be achieved by shaving the beam flanges [22,27,46,74]. Note that this research and development was conducted on deep beam sections without the presence of an axial load. Their application to bridge columns should proceed with caution.

39.3 Ductile Braced Frame Design

Seismic codesfor bridge design generally require that the primary energy dissipation mechanism be in the substructure. Braced frame systems, having considerable strength and stiffness, can be used for this purpose [67]. Depending on the geometry, a braced frame can be classified as either a concentrically braced frame (CBF) or an eccentrically braced frame (EBF). CBFs can be found in the cross-frames and lateral-bracing systems of many existing steel girder bridges. In a CBF system, the working lines of members essentially meet at a common point (Figure 39.7). Bracing members are prone to buckle inelastically under the cyclic compressive overloads. The consequence of cyclic buckling of brace members in the superstructure is not entirely known at this time, but some work has shown the importance of preserving the integrity of end-diaphragms [72]. Some seismic design recommendations [12] suggest that cross-frames and lateral bracing, which are part of the seismic force-resisting system in common slab-on-steel girder bridges, be designed to remain elastically under the imposed load effects. This issue is revisited in Section 39.5.

In a manner consistent with the earthquake-resistant design philosophy presented elsewhere in this chapter, modern CBFs are expected to undergo large inelastic deformation during a severe earthquake. Properly proportioned and detailed brace members can sustain these inelastic deformations and dissipate hysteretic energy in a stable manner through successive cycles of compression buckling and tension yielding. The preferred strategy is, therefore, to ensure that plastic deformation
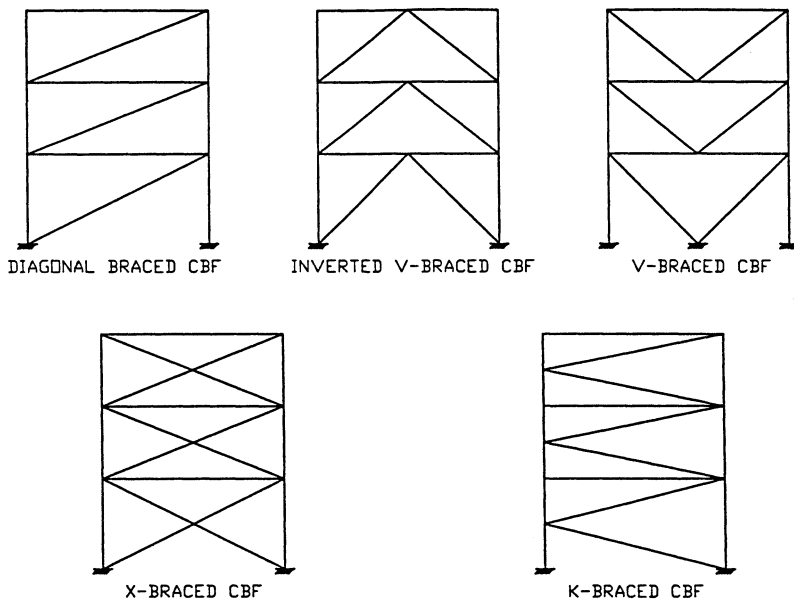
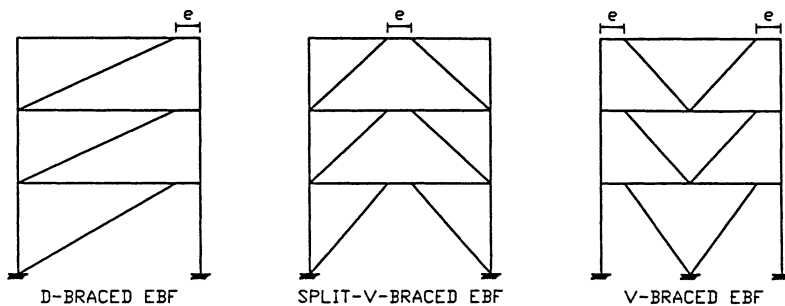**FIGURE 39.7**   Typical concentric bracing configurations.

FIGURE 39.8   Typical eccentric bracing configurations.

only occur in the braces, allowing the columns and beams to remain essentially elastic, thus maintaining the gravity load-carrying capacity during a major earthquake. According to the AISC Seismic Provisions [6], a CBF can be designed as either a special CBF (SCBF) or an ordinary CBF (OCBF). A large value of R is assigned to the SCBF system, but more stringent ductility detailing requirements need to be satisfied.

An EBF is a system of columns, beams, and braces in which at least one end of each bracing member connects to a beam at a short distance from its beam-to-column connection or from its adjacent beam-to-brace connection (Figure 39.8). The short segment of the beam between the brace connection and the column or between brace connections is called the link. Links in a properly designed EBF system will yield primarily in shear in a ductile manner. With minor modifications, the design provisions prescribed in the AISC Seismic Provisions for EBF, SCBF, and OCBF can be implemented for the seismic design of bridge substructures.

Current AASHTO seismic design provisions [3] do not prescribe the design seismic forces for the braced frame systems. For OCBFs, a response modification factor, R, of 2.0 is judged appropriate. For EBFs and SCBFs, an R value of 4 appears to be conservative and justifiable by examining the ductility reduction factor values prescribed in the building seismic design recommendations [57].

For CBFs, the emphasis in this chapter is placed on SCBFs, which are designed for better inelastic performance and energy dissipation capacity.

39.3.1 Concentrically Braced Frames

Tests have shown that, after buckling, an axially loaded member rapidly loses compressive strength under repeated inelastic load reversals and does not return to its original straight position (see Figure 39.4). CBFs exhibit the best seismic performance when both yielding in tension and inelastic buckling in compression of their diagonal members contribute significantly to the total hysteretic energy dissipation. The energy absorption capability of a brace in compression depends on its slenderness ratio (KL/r) and its resistance to local buckling. Since they are subjected to more stringent detailing requirements, SCBFs are expected to withstand significant inelastic deformations during a major earthquake. OCBFs are designed to higher levels of design seismic forces to minimize the extent of inelastic deformations. However, if an earthquake greater than that considered for design occurs, structures with SCBF could be greatly advantaged over the OCBF, in spite of the higher design force level considered in the latter case.

Bracing Members

Postbuckling strength and energy dissipation capacity of bracing members with a large slenderness ratio will degrade rapidly after buckling occurs [47]. Therefore, many seismic codes require the slenderness ratio (KL/r) for the bracing member be limited to $720/\sqrt{F_y}$, where F_y is in ksi. Recently, the AISC Seismic Provisions (1997) [6] have relaxed this limit to $1000/\sqrt{F_y}$ for bracing members in SCBFs. This change is somewhat controversial. The authors prefer to follow the more stringent past practice for SCBFs. The design strength of a bracing member in axial compression should be taken as $0.8\phi_c P_n$, where ϕ_c is taken as 0.85 and P_n is the nominal axial strength of the brace. The reduction factor of 0.8 has been prescribed for CBF systems in the previous seismic building provisions [6] to account for the degradation of compressive strength in the postbuckling region. The 1997 AISC Seismic Provisions have removed this reduction factor for SCBFs. But the authors still prefer to apply this strength reduction factor for the design of both SCBFs and OCBFs. Whenever the application of this reduction factor will lead to a less conservative design, however, such as to determine the maximum compressive force a bracing member imposes on adjacent structural elements, this reduction factor should not be used.

The plastic hinge that forms at midspan of a buckled brace may lead to severe local buckling. Large cyclic plastic strains that develop in the plastic hinge are likely to initiate fracture due to low-cycle fatigue. Therefore, the width–thickness ratio of stiffened or unstiffened elements of the brace section for SCBFs must be limited to the values specified in Table 39.2. The brace sections for OCBFs can be either compact or noncompact, but not slender. For brace members of angle, unstiffened rectangular, or hollow sections, the width–thickness ratios cannot exceed λ_{ps}.

To provide redundancy and to balance the tensile and compressive strengths in a CBF system, it is recommended that at least 30% but not more than 70% of the total seismic force be resisted by tension braces. This requirement can be waived if the bracing members are substantially oversized to provide essentially elastic seismic response.

Bracing Connections

The required strength of brace connections (including beam-to-column connections if part of the bracing system) should be able to resist the lesser of:

1. The expected axial tension strength ($= R_y F_y A_g$) of the brace.
2. The maximum force that can be transferred to the brace by the system.

In addition, the tensile strength of bracing members and their connections, based on the limit states of tensile rupture on the effective net section and block shear rupture, should be at least equal to the required strength of the brace as determined above.
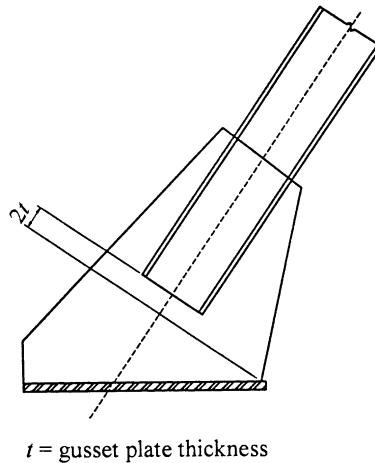
t = gusset plate thickness

FIGURE 39.9   Plastic hinge and free length of gusset plate.

End connections of the brace can be designed as either rigid or pin connection. For either of the end connection types, test results showed that the hysteresis responses are similar for a given *KL/r* [47]. When the brace is pin-connected and the brace is designed to buckle out of plane, it is suggested that the brace be terminated on the gusset a minimum of two times the gusset thickness from a line about which the gusset plate can bend unrestrained by the column or beam joints [6]. This condition is illustrated in Figure 39.9. The gusset plate should also be designed to carry the design compressive strength of the brace member without local buckling.

The effect of end fixity should be considered in determining the critical buckling axis if rigid end conditions are used for in-plane buckling and pinned connections are used for out-of-plane buckling. When analysis indicates that the brace will buckle in the plane of the braced frame, the design flexural strength of the connection should be equal to or greater than the expected flexural strength ($= 1.1R_yM_p$) of the brace. An exception to this requirement is permitted when the brace connections (1) meet the requirement of tensile rupture strength described above, (2) can accommodate the inelastic rotations associated with brace postbuckling deformations, and (3) have a design strength at least equal to the nominal compressive strength ($= A_gF_y$) of the brace.

Special Requirements for Brace Configuration

Because braces meet at the midspan of beams in V-type and inverted-V-type braced frames, the vertical force resulting from the unequal compression and tension strengths of the braces can have a considerable impact on cyclic behavior. Therefore, when this type of brace configuration is considered for SCBFs, the AISC Seismic Provisions require that:

1. A beam that is intersected by braces be continuous between columns.
2. A beam that is intersected by braces be designed to support the effects of all the prescribed tributary gravity loads assuming that the bracing is not present.
3. A beam that is intersected by braces be designed to resist the prescribed force effects incorporating an unbalanced vertical seismic force. This unbalanced seismic load must be substituted for the seismic force effect in the load combinations, and is the maximum unbalanced vertical force applied to the beam by the braces. It should be calculated using a minimum of P_y for the brace in tension and a maximum of $0.3 \phi_c P_n$ for the brace in compression. This requirement ensures that the beam will not fail due to the large unbalanced force after brace buckling.
4. The top and bottom flanges of the beam at the point of intersection of braces must be adequately braced; the lateral bracing should be designed for 2% of the nominal beam flange strength ($= F_yb_ft_{bf}$).

For OCBFs, the AISC Seismic Provisions waive the third requirement. But the brace members need to be designed for 1.5 times the required strength computed from the prescribed load combinations.

Columns

Based on the capacity design principle, columns in a CBF must be designed to remain elastic when all braces have reached their maximum tension or compression capacity considering an overstrength factor of $1.1R_y$. The AISC Seismic Provisions also require that columns satisfy the λps requirements (see Table 39.2). The strength of column splices must be designed to resist the imposed load effects. Partial penetration groove welds in the column splice have been experimentally observed to fail in a brittle manner [17]. Therefore, the AISC Seismic Provisions require that such splices in SCBFs be designed for at least 200% of the required strength, and be constructed with a minimum strength of 50% of the expected column strength, $R_y F_y A$, where A is the cross-sectional area of the smaller column connected. The column splice should be designed to develop both the nominal shear strength and 50% of the nominal flexural strength of the smaller section connected. Splices should be located in the middle one-third of the clear height of the column.

39.3.2 Eccentrically Braced Frames

Research results have shown that a well-designed EBF system possesses high stiffness in the elastic range and excellent ductility capacity in the inelastic range [25]. The high elastic stiffness is provided by the braces and the high ductility capacity is achieved by transmitting one brace force to another brace or to a column through shear and bending in a short beam segment designated as a "link." Figure 39.8 shows some typical arrangements of EBFs. In the figure, the link lengths are identified by the letter e. When properly detailed, these links provide a reliable source of energy dissipation. Following the capacity design concept, buckling of braces and beams outside of the link can be prevented by designing these members to remain elastic while resisting forces associated with the fully yielded and strain-hardened links. The AISC Seismic Provisions (1997) [6] for the EBF design are intended to achieve this objective.

Links

Figure 39.10 shows the free-body diagram of a link. If a link is short, the entire link yields primarily in shear. For a long link, flexural (or moment) hinge would form at both ends of the link before the "shear" hinge can be developed. A short link is desired for an efficient EBF design. In order to ensure stable yielding, links should be plastic sections satisfying the width–thickness ratios λps given in Table 39.2. Doubler plates welded to the link web should not be used as they do not perform as intended when subjected to large inelastic deformations. Openings should also be avoided as they adversely affect the yielding of the link web. The required shear strength, V_u, resulting from the prescribed load effects should not exceed the design shear strength of the link, ϕV_n, where $\phi = 0.9$. The nominal shear strength of the link is

$$V_n = \min \{V_p, \ 2M_p/e\} \tag{39.7}$$

$$V_p = 0.60F_y A_w \tag{39.8}$$

where $A_w = (d - 2t_f)t_w$.

A large axial force in the link will reduce the energy dissipation capacity. Therefore, its effect shall be considered by reducing the design shear strength and the link length. If the required link axial strength, Pu, resulting from the prescribed seismic effect exceeds $0.15P_y$, where $P_y = A_g F_y$, the following additional requirements should be met:
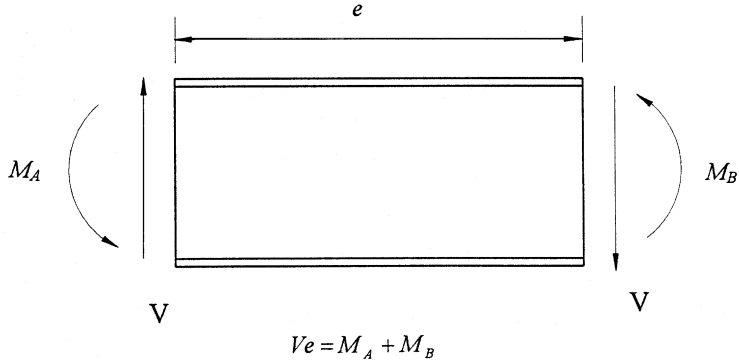
FIGURE 39.10 Static equilibrium of link.

1. The link design shear strength, ϕV_n, should be the lesser of ϕVpa or $2\phi M_{Pa}/e$, where V_{pa} and M_{Pa} are the reduced shear and flexural strengths, respectively:

$$V_{pa} = V_p\sqrt{1-(P_u/P_y)^2} \tag{39.9}$$

$$M_{Pa} = 1.18M_p[1-P_u/P_y)] \tag{39.10}$$

2. The length of the link should not exceed:

$$[1.15 - 0.5\,\rho'\,(A_w/A_g)]1.6M_p/V_p \qquad \text{for } \rho'\,(A_w/A_g) \geq 0.3 \tag{39.11}$$

$$1.6M_p/V_p \qquad\qquad\qquad \text{for } \rho'\,(A_w/A_g) < 0.3 \tag{39.12}$$

where $\rho' = P_u/V_u$.

The link rotation angle, γ, is the inelastic angle between the link and the beam outside of the link. The link rotation angle can be conservatively determined assuming that the braced bay will deform in a rigid–plastic mechanism. The plastic mechanism for one EBF configuration is illustrated in Figure 39.11. The plastic rotation is determined using a frame drift angle, θ_p, computed from the maximum frame displacement. Conservatively ignoring the elastic frame displacement, the plastic frame drift angle is $\theta_p = \delta/h$, where δ is the maximum displacement and h is the frame height.

Links yielding in shear possess a greater rotational capacity than links yielding in bending. For a link with a length of $1.6M_p/V_p$ or shorter (i.e., shear links), the link rotational demand should not exceed 0.08 rad. For a link with a length of $2.6M_p/V_p$ or longer (i.e., flexural links), the link rotational angle should not exceed 0.02 rad. A straight-line interpolation can be used to determine the link rotation capacity for the intermediate link length.

Link Stiffeners

In order to provide ductile behavior under severe cyclic loading, close attention to the detailing of link web stiffeners is required. At the brace end of the link, full-depth web stiffeners should be provided on both sides of the link web. These stiffeners should have a combined width not less than $(b_f - 2t_w)$, and a thickness not less than $0.75t_w$ nor ⅜ in. (10 mm), whichever is larger, where b_f and t_w are the link flange width and web thickness, respectively. In order to delay the link web or flange buckling, intermediate link web stiffeners should be provided as follows.
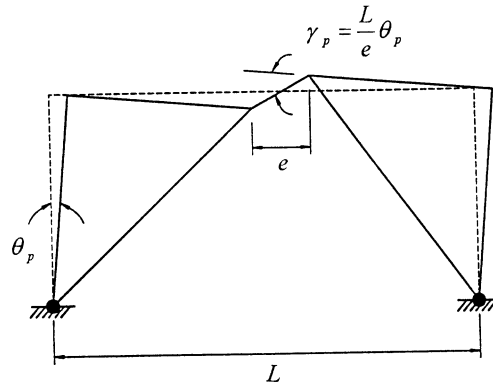
FIGURE 39.11   Energy dissipation mechanism of an eccentric braced frame.

1. In shear links, the spacing of intermediate web stiffeners depends on the magnitude of the link rotational demand. For links of lengths $1.6M_p/V_p$ or less, the intermediate web stiffener spacing should not exceed $(30t_w - d/5)$ for a link rotation angle of 0.08 rad, or $(52tw - d/5)$ for link rotation angles of 0.02 rad or less. Linear interpolation should be used for values between 0.08 and 0.02 rad.
2. Flexural links having lengths greater than $2.6M_p/V_p$ but less than $5M_p/V_p$ should have intermediate stiffeners at a distance from each link end equal to 1.5 times the beam flange width. Links between shear and flexural limits should have intermediate stiffeners meeting the requirements of both shear and flexural links. If link lengths are greater than $5M_p/V_p$, no intermediate stiffeners are required.
3. Intermediate stiffeners shall be full depth in order to react effectively against shear buckling. For links less than 25 in. deep, the stiffeners can be on one side only. The thickness of one-sided stiffeners should not be less than tw or ⅜ in., whichever is larger, and the width should not be less than $(b_f/2) - t_w$.
4. Fillet welds connecting a link stiffener to the link web should have a design strength adequate to resist a force of $A_{st}F_y$, where A_{st} is the area of the stiffener. The design strength of fillet welds connecting the stiffener to the flange should be adequate to resist a force of $A_{st}F_y/4$.

Link-to-Column Connections

Unless a very short shear link is used, large flexural demand in conjunction with high shear can develop at the link-to-column connections [25,63]. In light of the moment connection fractures observed after the Northridge earthquake, concerns have been raised on the seismic performance of link-to-column connections during a major earthquake. As a result, the AISC Seismic Provisions (1997) [6] require that the link-to-column design be based upon cyclic test results. Tests should follow specific loading procedures and results demonstrate an inelastic rotation capacity which is 20% greater than that computed in design. To avoid link-to-column connections, it is recommended that configuring the link between two braces be considered for EBF systems.

Lateral Support of Link

In order to assure stable behavior of the EBF system, it is essential to provide lateral support at both the top and bottom link flanges at the ends of the link. Each lateral support should have a design strength of 6% of the expected link flange strength ($= R_yF_yb_ft_f$).

Diagonal Brace and Beam outside of Link

Following the capacity design concept, diagonal braces and beam segments outside of the link should be designed to resist the maximum forces that can be generated by the link. Considering
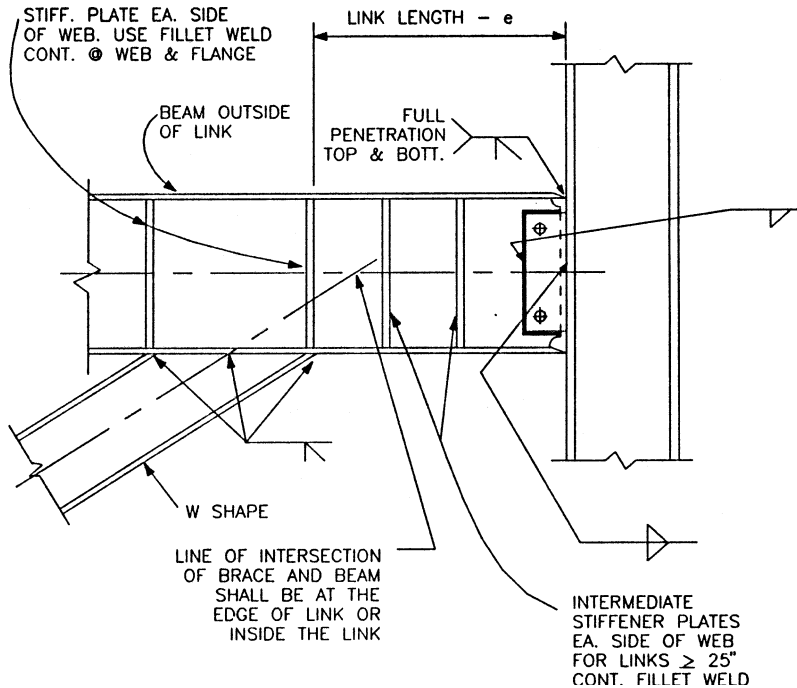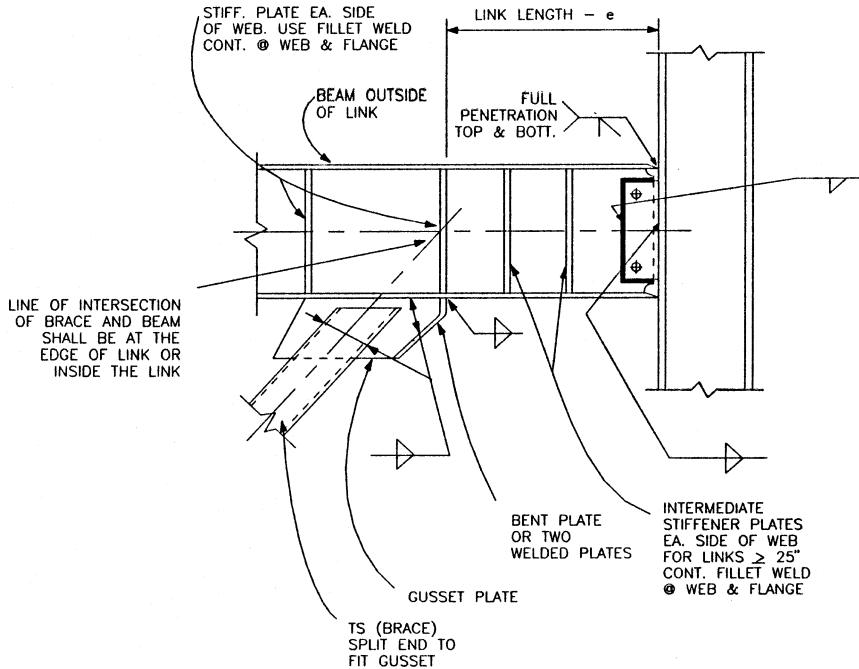
FIGURE 39.12 Diagonal brace fully connected to link. (Source: *AISC, Seismic Provisions for Structural Steel Buildings*; AISC, Chicago, IL, 1992. With permission.)

the strain-hardening effects, the required strength of the diagonal brace should be greater than the axial force and moment generated by 1.25 times the expected nominal shear strength of the link, $R_y V_n$.

The required strength of the beam outside of the link should be greater than the forces generated by 1.1 times the expected nominal shear strength of the link. To determine the beam design strength, it is permitted to multiply the beam design strength by the factor R_y. The link shear force will generate axial force in the diagonal brace. For most EBF configurations, the horizontal component of the brace force also generates a substantial axial force in the beam segment outside of the link. Since the brace and the beam outside of the link are designed to remain essentially elastic, the ratio of beam or brace axial force to link shear force is controlled primarily by the geometry of the EBF. This ratio is not much affected by the inelastic activity within the link; therefore, the ratio obtained from an elastic analysis can be used to scale up the beam and brace axial forces to a level corresponding to the link shear force specified above.

The link end moment is balanced by the brace and the beam outside of the link. If the brace connection at the link is designed as a pin, the beam by itself should be adequate to resist the entire link end moment. If the brace is considered to resist a portion of the link end moment, then the brace connection at the link should be designed as fully restrained. If used, lateral bracing of the beam should be provided at the beam top and bottom flanges. Each lateral bracing should have a required strength of 2% of the beam flange nominal strength, $F_y b_f t_f$. The required strength of the diagonal brace-to-beam connection at the link end of the brace should be at least the expected nominal strength of the brace. At the connection between the diagonal brace and the beam at the link end, the intersection of the brace and the beam centerlines should be at the end of the link or in the link (Figures 39.12 and 39.13). If the intersection of the brace and beam centerlines is located outside of the link, it will increase the bending moment generated in the beam and brace. The width–thickness ratio of the brace should satisfy λ_p specified in Table 39.2.

FIGURE 39.13 Diagonal brace pin-connected to link. (Source: AISC, *Seismic Provisions for Structural Steel Buildings*, AISC, Chicago, IL, 1992. With permission.)

Beam-to-Column Connections

Beam-to-column connections away from the links can be designed as simple shear connections. However, the connection must have a strength adequate to resist a rotation about the longitudinal axis of the beam resulting from two equal and opposite forces of at least 2% of the beam flange nominal strength, computed as $F_y b_f t_f$, and acting laterally on the beam flanges.

Required Column Strength

The required column strength should be determined from the prescribed load combinations, except that the moments and the axial loads introduced into the column at the connection of a link or brace should not be less than those generated by the expected nominal strength of the link, $RyVn$, multiplied by 1.1 to account for strain hardening. In addition to resisting the prescribed load effects, the design strength and the details of column splices must follow the recommendations given for the SCBFs.

39.4 Stiffened Steel Box Pier Design

39.4.1 Introduction

When space limitations dictate the use of a smaller-size bridge piers, steel box or circular sections gain an advantage over the reinforced concrete alternative. For circular or unstiffened box sections, the ductile detailing provisions of the AISC Seismic Provisions (1997) [6] or CHBDC [21] shall apply, including the diameter-to-thickness or width-to-thickness limits. For a box column of large dimensions, however, it is also possible to stiffen the wall plates by adding longitudinal and transverse stiffeners inside the section.

Design provisions for a stiffened box column are not covered in either the AASHTO or AISC design specifications. But the design and construction of this type of bridge pier has been common
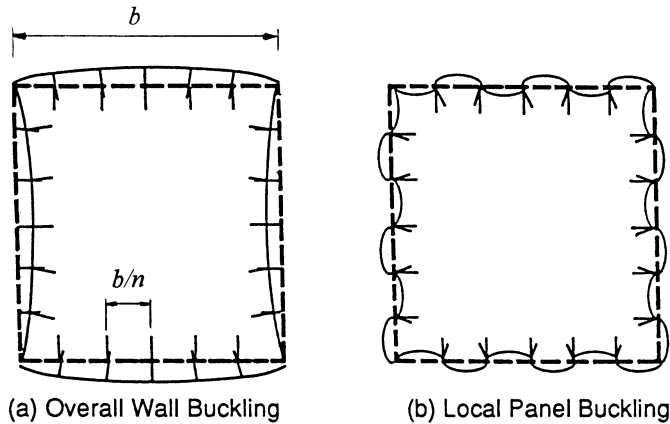
FIGURE 39.14 Buckling modes of box column with multiple stiffeners. (Source: Kawashima, K. et al., in *Stability and Ductility on Steel Structures under Cyclic Loading*; Fulsomoto, Y. and G. Lee, Eds., CRC, Boca Raton, FL, 1992. With permission.)

in Japan for more than 30 years. In the sections that follow, the basic behavior of stiffened plates is briefly reviewed. Next, design provisions contained in the Japanese Specifications for Highway Bridges [31] are presented. Results from an experimental investigation, conducted prior to the 1995 Hyogo-ken Nanbu earthquake in Japan, on cyclic performance of stiffened box piers are then used to evaluate the deformation capacity. Finally, lessons learned from the observed performance of this type of piers from the Hyogo-ken Nanbu earthquake are presented.

39.4.2 Stability of Rectangular Stiffened Box Piers

Three types of buckling modes can occur in a stiffened box pier. First, the plate segments between the longitudinal stiffeners may buckle, the stiffeners acting as nodal points (Figure 39.14b). In this type of "panel buckling," buckled waves appear on the surface of the piers, but the stiffeners do not appreciably move perpendicularly to the plate. Second, the entire stiffened box wall can globally buckle (Figure 39.14a). In this type of "wall buckling," the plate and stiffeners move together perpendicularly to the original plate plane. Third, the stiffeners themselves may buckle first, triggering in turn other buckling modes.

In Japan, a design criterion was developed following an extensive program of testing of stiffened steel plates in the 1960s and 1970s [70]; the results of this testing effort are shown in Figure 39.15, along with a best-fit curve. The slenderness parameter that defines the abscissa in the figure deserves some explanation. Realizing that the critical buckling stress of plate panels between longitudinal stiffeners can be obtained by the well-known result from the theory of elastic plate buckling:

$$F_{cr} = \frac{k_o \pi^2 E}{12(1-\nu^2)(b/nt)^2} \tag{39.13}$$

a normalized panel slenderness factor can be defined as

$$R_P = \sqrt{\frac{F_y}{F_{cr}}} = \left(\frac{b}{nt}\right)\sqrt{\frac{12 \ (1-\nu^2) \ F_y}{k_o \ \pi^2 E}} \tag{39.14}$$

where b and t are the stiffened plate width and thickness, respectively, n is the number of panel spaces in the plate (i.e., one more than the number of internal longitudinal stiffeners across the
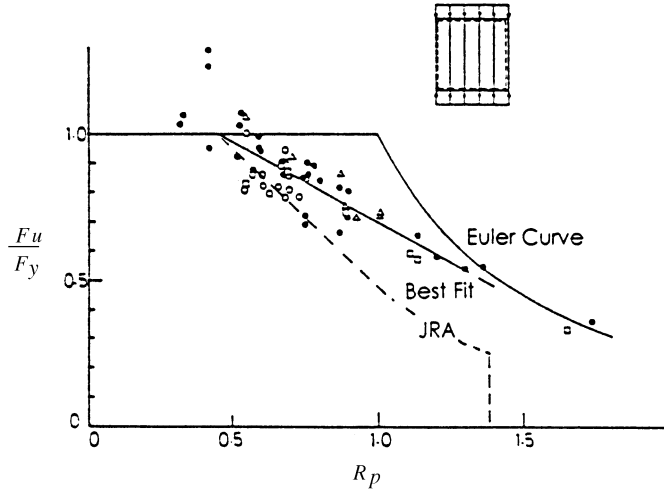
FIGURE 39.15 Relationship between buckling stress and R_p of stiffened plate.

plate), E is Young's modulus, ν is Poisson's ratio (0.3 for steel), and k_o (= 4 in. this case) is a factor taking into account the boundary conditions. The Japanese design requirement for stiffened plates in compression was based on a simplified and conservative curve obtained from the experimental data (see Figure 39.15):

$$
\begin{aligned}
\frac{F_u}{F_y} &= 1.0 && \text{for } R_p \leq 0.5 \\
\frac{F_u}{F_y} &= 1.5 - R_P && \text{for } 0.5 < R_P \leq 1.0 \\
\frac{F_u}{F_y} &= \frac{0.5}{R_P^2} && \text{for } R_P > 1.0
\end{aligned}
\tag{39.15}
$$

where Fu is the buckling strength.

Note that values of F_u/F_y less than 0.25 are not permitted. This expression is then converted into the allowable stress format of the Japanese bridge code, using a safety factor of 1.7. However, as allowable stresses are magnified by a factor of 1.7 for load combinations which include earthquake effects, the above ultimate strength expressions are effectively used.

The point $R_p = 0.5$ defines the theoretical boundary between the region where the yield stress can be reached prior to local buckling ($R_p < 0.5$), and vice versa ($R_p \geq 0.5$). For a given steel grade, Eq. (39.14) for $R_p = 0.5$ corresponds to a limiting b/nt ratio:

$$
\left(\frac{b}{nt}\right)_o = \frac{162}{\sqrt{F_y}}
\tag{39.16}
$$

and for a given plate width, b, the "critical thickness," t_o, is

$$
t_o = \frac{b\sqrt{F_y}}{162n}
\tag{39.17}
$$

where F_y is in ksi. That is, for a stiffened box column of a given width, using a plate thicker than t_o will ensure yielding prior to panel buckling.

To be able to design the longitudinal stiffeners, it is necessary to define two additional parameters: the stiffness ratio of a longitudinal stiffener to a plate, γ_l, and the corresponding area ratio, δ_l. As the name implies:

$$\gamma_l = \frac{\text{stiffener flexural rigidity}}{\text{plate flexural rigidity}} = \frac{EI_l}{bD} = \frac{12\,(1\,-\,\nu^2)\,I_l}{bt^3} = \frac{10.92\,I_l}{b\,t^3} \approx \frac{11\,I_l}{b\,t^3} \quad (39.18)$$

where I_l is the moment of inertia of the T-section made up of a longitudinal stiffener and the effective width of the plate to which it connects (or, more conservatively and expediently, the moment of inertia of a longitudinal stiffener taken about the axis located at the inside face of the stiffened plate). Similarly, the area ratio is expressed as

$$\delta_l = \frac{\text{stiffener axial rigidity}}{\text{plate axial rigidity}} = \frac{A_l}{bt} \quad (39.19)$$

where A_l is the area of a longitudinal stiffener.

Since the purpose of adding stiffeners to a box section is partly to eliminate the severity of wall buckling, there exists an "optimum rigidity," γ_l^*, of the stiffeners beyond which panel buckling between the stiffeners will develop before wall buckling. In principle, according to elastic buckling theory for ideal plates (i.e., plates without geometric imperfections and residual stresses), further increases in rigidity beyond that optimum would not further enhance the buckling capacity of the box pier. Although more complex definitions of this parameter exist in the literature [35], the above description is generally sufficient for the box piers of interest here. This optimum rigidity is:

$$\gamma_l^* = 4\alpha^2 n\,(\,1\,+\,n\delta_l\,) - \frac{(\alpha^2\,+\,1)^2}{n} \qquad \text{for } \alpha \leq \alpha_o \quad (39.20)$$

and

$$\gamma_l^* = \frac{1}{n}\left\{\left[\,2\,n^2\,(\,1\,+\,n\delta_l\,)-1\,\right]^2 -1\right\} \qquad \text{for } \alpha > \alpha_o \quad (39.21)$$

where α is the aspect ratio, a/b, a being the spacing between the transverse stiffeners (or diaphragms), and the critical aspect ratio α_o is defined as

$$\alpha_o = \sqrt[4]{1\,+\,n\,\gamma_l} \quad (39.22)$$

These expressions can be obtained by recognizing that, for plates of thickness less than t_o, it is logical to design the longitudinal stiffeners such that wall buckling does not occur prior to panel buckling and, consequently, as a minimum, be able to reach the same ultimate stress as the latter. Defining a normalized slenderness factor, R_H, for the stiffened plate:

$$R_H = \sqrt{\frac{F_y}{F_{cr}}} = \left(\frac{b}{t}\right)\sqrt{\frac{12\,(1-\nu^2)\,F_y}{k_s\,\pi^2 E}} \quad (39.23)$$

Based on elastic plate buckling theory, k_s for a stiffened plate is equal to [15]:

$$k_s = \frac{(1 + \alpha^2)^2 + n \gamma_l}{\alpha^2 (1 + n \delta_l)} \qquad \text{for } \alpha \le \alpha_o$$

$$k_s = \frac{2\left(1 + \sqrt{1 + n \gamma_l}\right)}{(1 + n \delta_l)} \qquad \text{for } \alpha > \alpha_o \qquad (39.24)$$

Letting $R_H = R_P$ (i.e, both wall buckling and panel buckling can develop the same ultimate stress), the expressions for γ_l^* in Eqs. (39.20) and (39.21) can be derived. Thus, when the stiffened plate thickness, t, is less t_o, the JRA Specifications specify that either Eq. (39.20) or (39.21) be used to determine the required stiffness of the longitudinal stiffeners.

When a plate thicker than t_o is chosen, however, larger stiffeners are unnecessary since yielding will occur prior to buckling. This means that the critical buckling stress for wall buckling does not need to exceed the yield stress, which is reached by the panel buckling when $t = t_o$. The panel slenderness ratio for $t = t_o$ is

$$R_{P(t=t_o)} = \frac{b}{nt_o} \sqrt{\frac{12(1 - v^2)F_y}{k_o \pi^2 E}} \qquad (39.25)$$

Equating R_P to R_H in Eq. (39.23), the required γ_l^* can be obtained as follows:

$$\gamma_l^* = 4\alpha^2 n \left(\frac{t_o}{t}\right)^2 (1 + n\delta_l) - \frac{(\alpha^2 + 1)^2}{n} \qquad \text{for } \alpha \le \alpha_o \qquad (39.26)$$

and

$$\gamma_l^* = \frac{1}{n}\left\{ \left[2 n^2 \left(\frac{t_o}{t}\right)^2 (1 + n\delta_l) - 1 \right]^2 - 1 \right\} \qquad \text{for } \alpha > \alpha_o \qquad (39.27)$$

It is noteworthy that the above requirements do not ensure ductile behavior of steel piers. To achieve higher ductility for seismic application in moderate to high seismic regions, it is prudent to limit t to t_o. In addition to the above requirements, conventional slenderness limits are imposed to prevent local buckling of the stiffeners prior to that of the main member. For example, when a flat bar is used, the limiting width–thickness ratio (λ_r) for the stiffeners is $95/\sqrt{F_y}$.

The JRA requirements for the design of stiffened box columns are summarized as follows.

1. At least two stiffeners of the steel grade no less than that of the plate are required. Stiffeners are to be equally spaced so that the stiffened plate is divided into n equal intervals. To consider the beneficial effect of the stress gradient, b/nt in Eq. (39.14) can be replaced by $b/nt\varphi$, where φ is computed as

$$\varphi = \frac{\sigma_1 - \sigma_2}{\sigma_1} \qquad (39.28)$$

In the above equation, σ_1 and σ_2 are the stresses at both edges of the plate; compressive stress is defined as positive, and $\sigma_1 > \sigma_2$. The value of φ is equal to 1 for uniform compression and 2 for equal and opposite stresses at both edges of the plate. Where the plastic hinge is expected to form, it is conservative to assume a φ value of 1.

2. Each longitudinal stiffener needs to have sufficient area and stiffness to prevent wall buckling. The minimum required area, in the form of an area ratio in Eq. (39.19), is

$$\left(\delta_l\right)_{\min} = \frac{1}{10n} \tag{39.29}$$

The minimum required moment of inertia, expressed in the form of stiffness ratio in Eq. (39.18), is determined as follows. When the following two requirements are satisfied, use either Eq. (39.26) for $t \geq t_o$ or Eq. (39.20) for $t < t_o$:

$$\alpha \leq \alpha_o \tag{39.30}$$

$$I_t \geq \frac{bt^3}{11}\left(\frac{1+n\gamma_l^*}{4\alpha^3}\right) \tag{39.31}$$

where It is the moment of inertia of the transverse stiffener, taken at the base of the stiffener. Otherwise, use either Eq. (39.27) for $t \geq t_o$ or Eq. (39.21) for $t < t_o$.

39.4.3   Japanese Research Prior to the 1995 Hyogo-ken Nanbu Earthquake

While large steel box bridge piers have been used in the construction of Japanese expressways for at least 30 years, research on their seismic resistance only started in the early 1980s. The first inelastic cyclic tests of thin-walled box piers were conducted by Usami and Fukumoto [65] as well as Fukumoto and Kusama [29]. Other tests were conducted by the Public Works Research Institute of the Ministry of Construction (e.g., Kawashima et al. [32]; MacRae and Kawashima [36]) and research groups at various universities (e.g., Watanabe et al. [69], Usami et al. [66], Nishimura et al. [45]).

The Public Work Research Institute tests considered 22 stiffened box piers of configuration representative of those used in some major Japanese expressways. The parameters considered in the investigation included the yield strength, weld size, loading type and sequence, stiffener type (flat bar vs. structural tree), and partial-height concrete infill. An axial load ranging from 7.8 to 11% of the axial yield load was applied to the cantilever specimens for cyclic testing. Typical hysteresis responses of one steel pier and one with concrete infill at the lower one-third of the pier height are shown in Figure 39.16. For bare steel specimens, test results showed that stiffened plates were able to yield and strain-harden. The average ratio between the maximum lateral strength and the predicted yield strength was about 1.4; the corresponding ratio between the maximum strength and plastic strength was about 1.2. The displacement ductility ranged between 3 and 5. Based on Eq. (39.2), the observed levels of ductility and structural overstrength imply that the response modification factor, R, for this type of pier can be conservatively taken as 3.5 ($\approx 1.2 \times 3$). Specimens with a γ_l / γ_l^* ratio less than 2.0 behaved in a wall-buckling mode with severe strength degradation. Otherwise, specimens exhibited local panel buckling.

Four of the 22 specimens were filled with concrete over the bottom one-third of their height. Prior to the Hyogo-ken Nanbu earthquake, it was not uncommon in Japan to fill bridge piers with concrete to reduce the damage which may occur as a result of a vehicle collision with the pier; generally the effect of the concrete infill was neglected in design calculations. It was thought prior to the testing that concrete infill would increase the deformation capacity because inward buckling of stiffened plates was inhibited.

Figure 39.17 compares the response envelopes of two identical specimens, except that one is with and the other one without concrete infill. For the concrete-filled specimen, little plate buckling was observed, and the lateral strength was about 30% higher than the bare steel specimen. Other than

(Specimen S1)

(a)

(b)
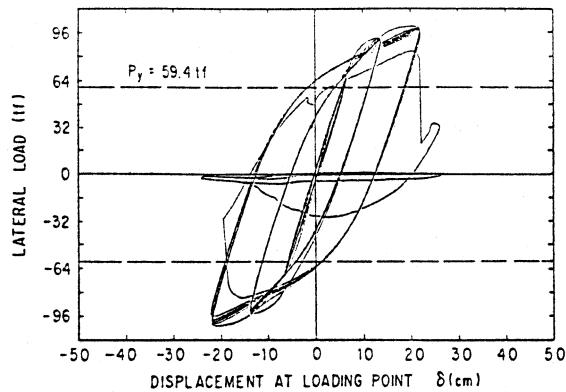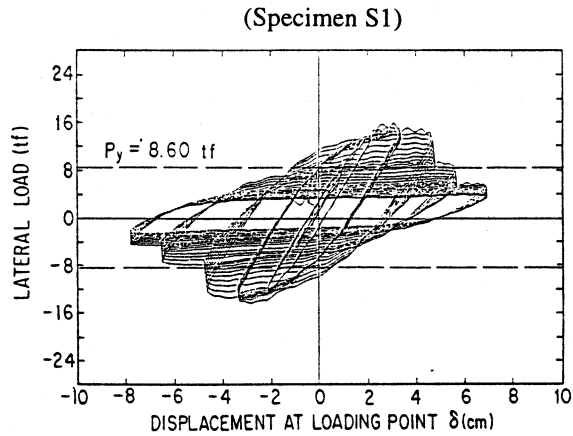
FIGURE 39.16 Hysteresis responses of two stiffened box piers. (Source: Kawashima, K. et al., in *Stability and Ductility on Steel Structures under Cyclic Loading*; Fulsomoto, Y. and G. Lee, Eds., CRC, Boca Raton, FL, 1992. With permission.)

exhibiting ductile buckling mode, all the concrete-filled specimens suffered brittle fracture in or around the weld at the pier base. See Figure 39.16b for a typical cyclic response. It appears that the composite effect, which not only increased the overall flexural strength but also caused a shift of the neutral axis, produced an overload to the welded joint. As a result, the ductility capacity was reduced by up to 23%. It appears from the test results that the welded connection at the pier base needs to be designed for the overstrength including the composite effect.

A large portion of the research effort in years shortly prior to the Hyogo-ken Nanbu earthquake investigated the effectiveness of many different strategies to improve the seismic performance, ductility, and energy dissipation of those steel piers [34,66,68]. Among the factors observed to have a beneficiary influence were the use of (1) a γ_l / γ_l^* ratio above 3 as a minimum, or preferably 5; (2) longitudinal stiffeners having a higher grade of steel than the box plates; (3) minimal amount of stiffeners; (4) concrete filling of steel piers; and (5) box columns having round corners, built from bend plates, and having weld seams away from the corners, thus avoiding the typically problem-prone sharp welded corners [69].
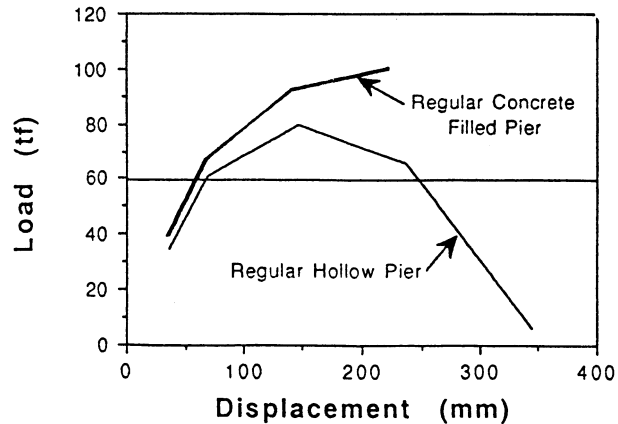
**FIGURE 39.17** Effect of infill on cyclic response envelopes. (Source: Kawashima, K. et al., 1992.)

39.4.4 Japanese Research after the 1995 Hyogo-ken Nanbu Earthquake

Steel bridge piers were severely tested during the 1995 Hyogo-ken Nanbu earthquake in Japan. Recorded ground motions in the area indicated that the earthquake of a magnitude 7.2 produced a peak ground velocity of about 90 cm/s (the peak ground acceleration was about a 0.8 *g*). Of all the steel bridge piers, about 1% experienced severe damage or even collapse. But about a half of the steel bridge piers were damaged to some degree.

In addition to wall buckling and panel buckling, damage at the pier base, in the form of weld fracture or plastic elongation of anchor bolts, was also observed. Based on the observed buckling patterns, Watanabe et al. [69] suggested that the width–thickness of the wall plate needs to be further reduced, and the required stiffness of stiffeners, γ_l^*, needs to be increased by three times.

After the Hyogo-ken Nanbu earthquake, filling concrete to existing steel piers, either damaged or nondamaged ones, was suggested to be one of the most effective means to strength stiffened box piers [23,41]. Figure 39.18 shows a typical example of the retrofit. As was demonstrated in Figure 39.17, concrete infill will increase the flexural strength of the pier, imposing a higher force demand to the foundation and connections (welds and anchor bolts) at the base of the pier. Therefore, the composite effect needs to be considered in retrofit design. The capacities of the foundation and base connections also need to be checked to ensure that the weakest part of the retrofitted structure is not in these regions. Since concrete infill would force the stiffened wall plates to buckle outward, the welded joint between wall plates is likely to experience higher stresses (see Figure 39.19).

Because concrete infill for seismic retrofit may introduce several undesirable effects, alternative solutions have been sought that would enhance the deformation capacity while keeping the strength increase to a minimum. Based on the observed buckling of stiffened plates that accounted for the majority of damage to rectangular piers, Nishikawa et al. [44] postulated that local buckling is not always the ultimate limit state. They observed that bridge piers experienced limited damages when the corners of the box section remained straight, but piers were badly deformed when corner welds that fractured could not maintain the corners straight. To demonstrate their concept, three retrofit schemes shown in Figure 39.20a were verified by cyclic testing. Specimen No. 3 was retrofitted by adding stiffeners. Box corners of Specimen No. 4 were strengthened by welding angles and corner plates, while the stiffening angles of Specimen No. 5 were bolted to stiffened wall plates. Response envelopes in Figure 39.20b indicate that Specimen No. 5 had the least increase in lateral strength above the nonretrofitted Specimen No. 2, yet the deformation capacity was comparable to other retrofitted specimens.
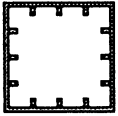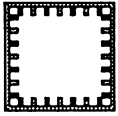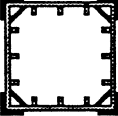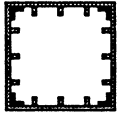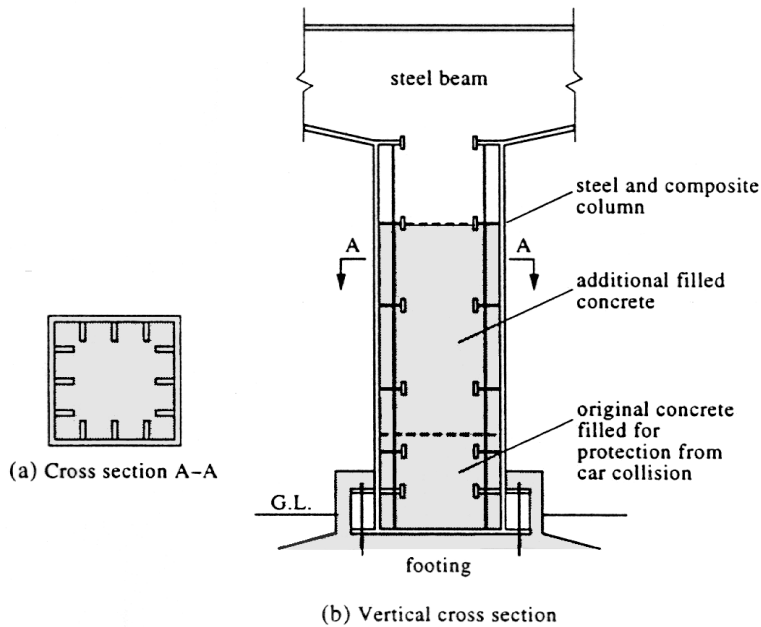
FIGURE 39.18 Retrofitted stiffened box pier with concrete infill. (Source: Fukumoto, Y. et al., in *Bridge Management*, Vol. 3, Thomas Telford, 1996. With permission.)
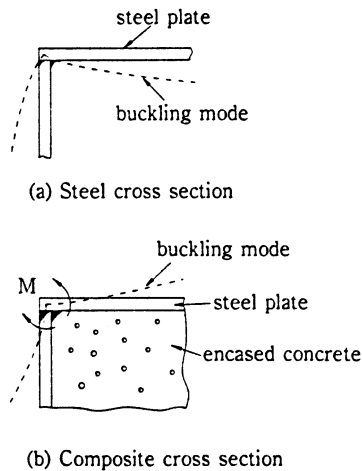

FIGURE 39.19 Effect of concrete infill on welded joint of stiffened box pier. (Source: Kitada, *Eng. Struct.*, 20(4–6), 347-354, 1998. With permission.)

39.5 Alternative Schemes

As described above, damage to substructure components such as abutments, piers, bearings, and others have proved to be of great consequence, often leading to span collapses [8,19,50]. Hence, when existing bridges are targeted for seismic rehabilitation, much attention needs to be paid to these substructure elements. Typically, the current retrofitting practice is to either strengthen or replace the existing nonductile members (e.g., ATC [10], Buckle et al. [20], Shirolé and Malik [58]),

No.	Section	Outline of retrofitting
2		No retrofitting (Basic section)
3		Addition of stiffeners (80x6mm)
4		Outer angle plates & (130x130x6mm) inner flat corner plates (170x6mm)
5		Inner angle plates (90x90x9mm)

(a)
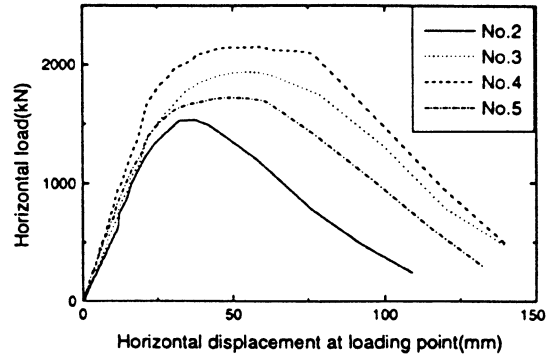
(b)

FIGURE 39.20 Seismic retrofit without concrete infill. (a) Retrofit schemes; (b) response envelopes. (Source: Nishikawa, K. et al, *Eng. Struct.*, 2062-6), 540-551, 1998. With permission.)

enhance the ductility capacity (e.g., Degenkolb [24], Priestley et al. [49]), or reduce the force demands on the vulnerable substructure elements using base isolation techniques or other structural modifications (e.g., Mayes et al. [38], Astaneh-Asl [7]). While all these approaches are proven effective, only the base isolation concept currently recognizes that seismic deficiency attributable to substructure weaknesses may be resolved by operating elsewhere than on the substructure itself. Moreover, all approaches can be costly, even base isolation in those instances when significant abutments modifications and other structural changes are needed to permit large displacements at the isolation bearings and lateral load redistribution among piers [39]. Thus, a seismic retrofit strategy that relies instead on ductile end diaphragms inserted in the steel superstructure, if effective, could provide an alternative.

Lateral load analyses have revealed the important role played by the end diaphragms in slab-on-girder steel bridges [72]. In absence of end diaphragms, girders severely distort at their supports, whether or not stiff intermediate diaphragms are present along the span. Because end diaphragms are key links along the load path for the inertia forces seismically induced at deck level, it might be possible, in some cases, to prevent damage from developing in the nonductile substructure (i.e., piers, foundation, and bearings) by replacing the steel diaphragms over abutments and piers with specially designed ductile diaphragms calibrated to yield before the strength of the substructure is reached. This objective is schematically illustrated in Figure 39.21 for slab-on-girder bridges and in Figure 39.22 for deck-truss bridges. In the latter case, however, ductile diaphragms must be inserted in the last lower lateral panels before the supports, in addition to the end diaphragms; in deck-truss bridges, seismically induced inertia forces in the transverse direction at deck level act with a sizable eccentricity with respect to the truss reaction supports, and the entire superstructure (top and lower lateral bracings, end and interior cross-frame bracings, and other lateral-load-resisting components) is mobilized to transfer these forces from deck to supports.

While conceptually simple, the implementation of ductile diaphragms in existing bridges requires consideration of many strength, stiffness, and drift constraints germane to the type of steel bridge
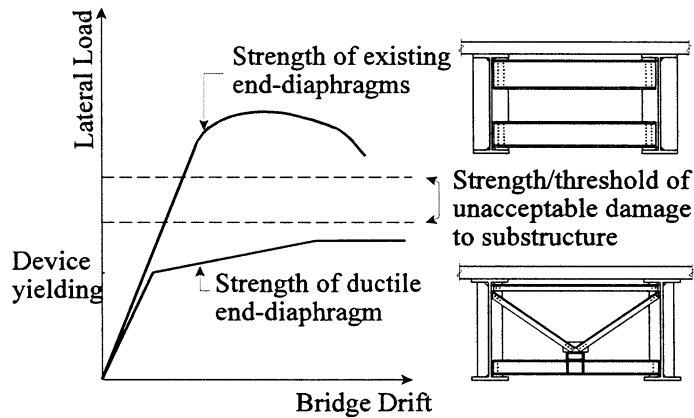
FIGURE 39.21   Schematic illustration of the ductile end-diaphragm concept.
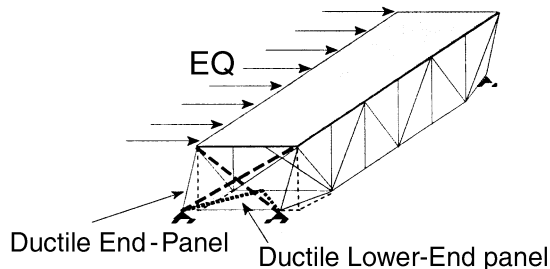

FIGURE 39.22   Ductile diaphragm retrofit concept in a deck-truss.

investigated. For example, for slab-on-girder bridges, because girders with large bearing stiffeners at the supports can contribute non-negligibly to the lateral strength of the bridges, stiff ductile diaphragms are preferred. Tests [73] confirmed that stiff welded ductile diaphragms are indeed more effective than bolted alternatives. As for deck-trusses, both upper and lower limits are imposed on the ductile diaphragm stiffnesses to satisfy maximum drifts and ductility requirements, and a systematic solution strategy is often necessary to achieve an acceptable retrofit [55,56].

Many types of systems capable of stable passive seismic energy dissipation could serve as ductile diaphragms. Among those, EBF presented in Section 39.3.2, shear panel systems (SPS) [28,40], and steel triangular-plate added damping and stiffness devices (TADAS) [61] have received particular attention in building applications. Still, to the authors' knowledge, none of these applications has been considered to date for bridge structures. This may be partly attributable to the absence of seismic design provisions in North American bridge codes. Examples of how these systems would be implemented in the end diaphragms of a typical 40-m span slab-on-girder bridge are shown in Figure 39.23. Similar implementations in deck-trusses are shown in Figure 39.24.

While the ductile diaphragm concept is promising and appears satisfactory for spans supported on stiff substructures based on the results available at the time of this writing, and could in fact be equally effective in new structures, more research is needed before common implementation is possible. In particular, large-scale experimental verification of the concept and expected behavior is desirable; parametric studies to investigate the range of substructure stiffnesses for which this retrofit strategy can be effective are also needed. It should also be noted that this concept only provides enhanced seismic resistance and substructure protection for the component of seismic excitation transverse to the bridge, and must be coupled with other devices that constrain longitudinal seismic displacements, such as simple bearings strengthening [37], rubber bumpers, and the
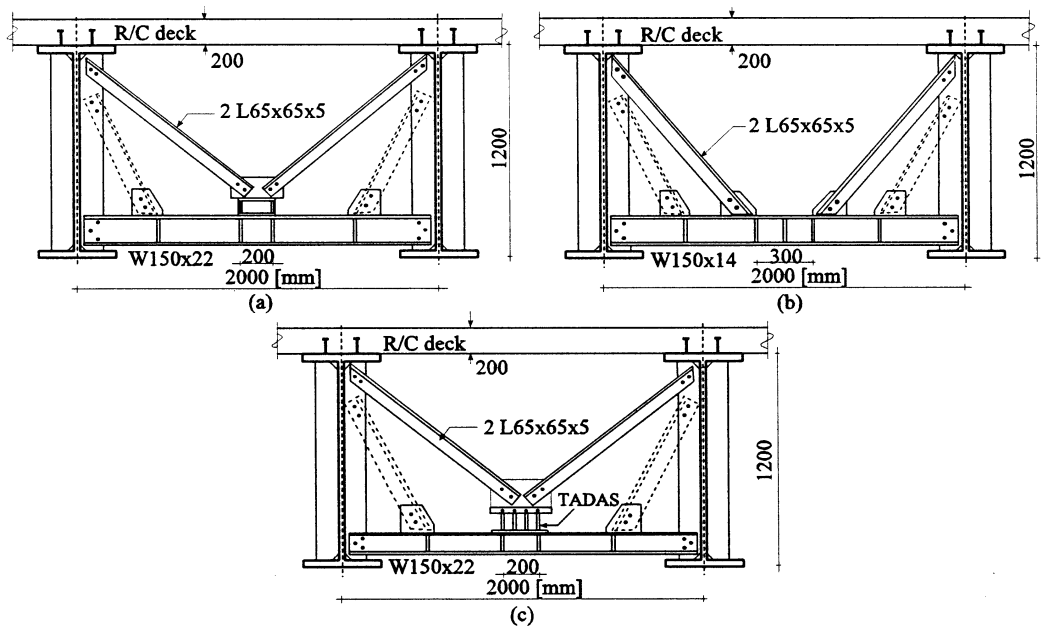
FIGURE 39.23 Ductile end diaphragm in a typical 40-m-span bridge (a) SPS; (b) EBF; (c) TADAS. (Other unbraced girders not shown; dotted members only if required for jacking purposes for nonseismic reasons).
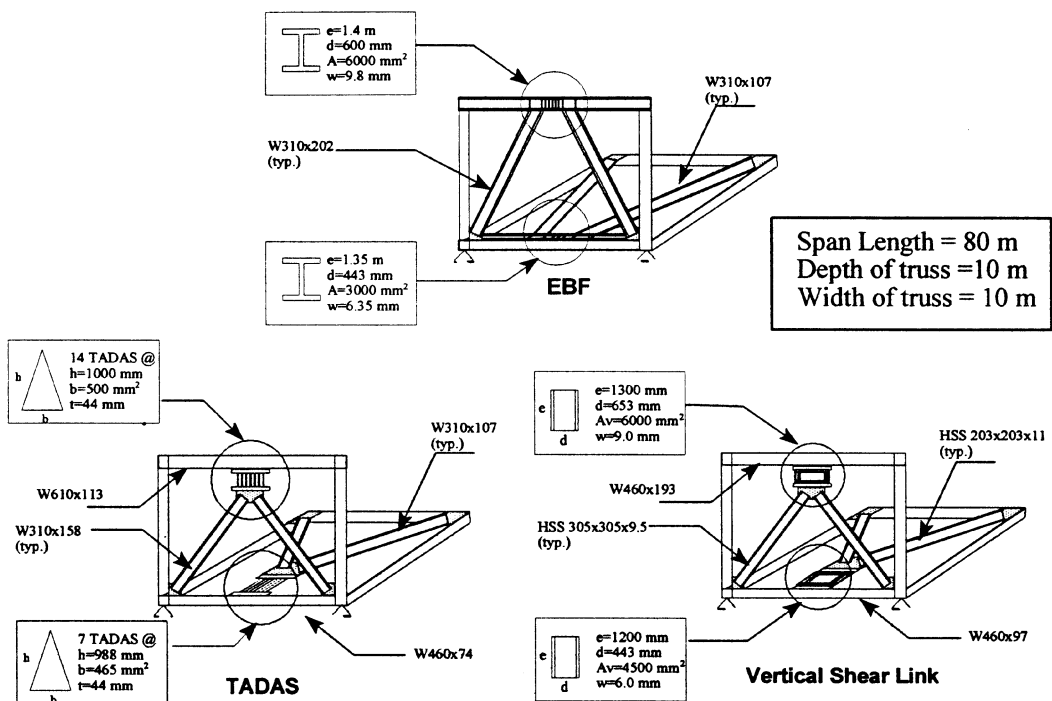

FIGURE 39.24 Examples of ductile retrofit systems at span end of deck-trusses.

like. Transportation agencies experienced in seismic bridge retrofit have indicated that deficiencies in the longitudinal direction of these bridges are typically easier to address than those in the lateral direction.

References

1. AASHTO, *LRFD Bridge Design Specifications*, American Association of State Highways and Transportaion Officials, Washington, D.C., 1994.
2. AASHTO, *Standard Specifications for Highway Bridges*, AASHTO, Washington, D.C., 1996.
3. AASHTO, *Standard Specifications for Seismic Design of Highway Bridges*, Washington, D.C., 1992.
4. AISC, Commentary on highly restrained welded connections, *Eng. J. AISC,* 10(3), 61–73, 1973.
5. AISC, *Load and Resistance Factor Design Specification for Structural Steel Buildings*, AISC, Chicago, IL, 1993.
6. AISC, *Seismic Provisions for Structural Steel Buildings,* AISC, Chicago, IL, 1992 and 1997.
7. Astaneh-Asl, A., Seismic retrofit concepts for the East Bay Crossing of the San Francisco–Oakland Bay Bridge," in *Proc. 1st U.S. Seminar on Seismic Evaluation and Retrofit of Steel Bridges,* San Francisco, CA, 1993.
8. Astaneh-Asl, A., Bolt, B., Mcmullin, K. M., Donikian, R. R., Modjtahedi, D., and Cho, S. W., Seismic Performance of Steel Bridges during the 1994 Northridge Earthquake, Report No. CE-STEEL 94/01, Berkeley, CA, 1994.
9. ATC, Tentative Provisions for the Development of Seismic Design Provisions for Buildings, Report No. ATC 3-06, Applied Technology Council, Palo Alto, CA, 1978.
10. ATC, Seismic Retrofitting Guidelines for Highway Bridges, *Report No. ATC-6-2,* Applied Technology Council, Palo Alto, CA, 1983.
11. ATC, Seismic Design Criteria for Highway Structures, *Report No. ATC-18*, Applied Technology Council, Redwood, CA,1996.
12. ATC, Improved Seismic Design Criteria for California Bridges: Provisional Recommendations, *Report No. ATC-32*, Applied Technology Council, Redwood, CA,1996.
13. AWS, *Structural Welding Code — Steel*, ANSI/AWS D1.1-98, AWS, Miami, FL, 1998.
14. AWS, *Bridge Welding Code*, ANSI/AWS D1.5-96, AWS, Miami, FL, 1996.
15. Ballio, G. and Mazzolani, F. M., *Theory and Design of Steel Structures.* Chapman and Hall, New York, 632 pp, 1983.
16. Blodgett, O. W. and Miller, D. K., Special welding issues for seismically resistant structures, in *Steel Design Handbook*, A. R. Tamboli, Ed., McGraw-Hill, New York, 1997.
17. Bruneau, M. and Mahin, S. A., Ultimate behavior of heavy steel section welded splices and design implications, *J. Struct. Eng. ASCE,* 116(8), 2214–2235, 1990.
18. Bruneau, M., Uang, C.-M., and Whittaker, A., *Ductile Design of Steel Structures*, McGraw-Hill, New York, 1997.
19. Bruneau, M., Wilson, J. W., and Tremblay, R., Performance of steel bridges during the 1995 Hyogo-ken-Nanbu (Kobe, Japan) earthquake, *Can. J. Civ. Eng.*, 23(3), 678–713, 1996.
20. Buckle, I. G., Mayes, R. L., and Button, M. R., Seismic Design and Retrofit Manual for Highway Bridges, Report No. FHWA-IP-87-6, U.S. Department of Transportation, Federal Highway Administration, 1986.
21. CHBDC, Canadian Highway Bridge Design Code, Seismic Provisions, Seismic Committee of the CHBDC, Rexdale, Ontario, Canada, 1998.
22. Chen, S. J., Yeh, C. H., and Chu, J. M., Ductile steel beam-column connections for seismic resistance, *J. Struct. Eng.*, *ASCE,* 122(11), 1292–1299; 1996.
23. Committee on Roadway Bridges by the Hyogoken-Nanbu Earthquake, *Specifications on Retrofitting of Damaged Roadway Bridges by the Hyogoken-Nanbu Earthquake*, 1995. [in Japanese].
24. Degenkolb, O. H., Retrofitting bridges to increase seismic resistance, *J. Tech. Councils ASCE,* 104(TC1), 13–20, 1978.

25. Popov, E. P., Engelhardt, M. D., and Ricles, J. M., Eccentrically braced frames: U.S. practice, *Eng. J. AISC,* 26(2), 66–80, 1989.

26. Engelhardt, M. D. and Sabol, T., Reinforcing of steel moment connections with cover plates: benefits and limitations, *Eng. Struct.,* 20(4–6), 510–520, 1998.

27. Engelhardt, M. D., Winneburger, T., Zekany, A. J., and Potyraj, T. J., "The dogbone connection: Part II, *Modern Steel Construction, AISC,* 36(8), pp. 46–55, 1996.

28. Fehling, E., Pauli, W. and Bouwkamp, J. G., Use of vertical shear-links in eccentrically braced frames, *Proc. 10th World Conf. on Earthquake Eng.,* Madrid, Vol. 9, 1992, 4475–4479.

29. Fukumoto, Y. and Kusama, H., Cyclic bending tests of thin-walled box beams, *Proc. JSCE Struct. Eng./Earthquake Eng.,* 2(1), 117s–127s, 1985.

30. Fukumoto, Y., Watanabe, E., Kitada, T., Suzuki, I., Horie, Y., and Sakoda, H., Reconstruction and repair of steel highway bridges damaged by the Great Hanshin earthquake, in *Bridge Management,* Vol. 3, Thomas Telford, 1996, 8–16.

31. JRA, Specifications of Highway Bridges, Japan Road Association, Tokyo, Japan, 1996.

32. Kawashima, K., MacRae, G., Hasegawa, K., Ikeuchi, T., and Kazuya, O., Ductility of steel bridge piers from dynamic loading tests, in *Stability and Ductility of Steel Structures under Cyclic Loading,* Fukomoto, Y. and G. Lee, Eds., CRC Press, Boca Raton, FL, 1992.

33. Kitada, T., Ultimate strength and ductility of state-of-the-art concrete-filled steel bridge piers in Japan, *Eng. Struct.,* 20(4–6), 347–354, 1998.

34. Kitada, T., Nanjo, A., and Okashiro, S., Limit states and design methods considering ductility of steel piers for bridges under seismic load, in *Proc., 5th East Asia-Pacific Conference on Structural Engineering and Construction,* Queensland, Australia, 1995.

35. Kristek, V. and Skaloud, M., *Advanced Analysis and Design of Plated Structures, Developments in Civil Engineering,* Vol. 32, Elsevier, New York, 1991, 333 pp.

36. MacRae, G. and Kawashima, K., Estimation of the deformation capacity of steel bridge piers, in *Stability and Ductility of Steel Structures under Cyclic Loading,* Fukomoto, Y. and G. Lee, Eds., CRC Press, Boca Raton, FL, 1992.

37. Mander, J. B., Kim, D.-K., Chen, S. S., and Premus, G. J., Response of Steel Bridge Bearings to Reversed Cyclic Loading, Report No. NCEER-96-0014, State University of New York, Buffalo, 1996.

38. Mayes, R. L., Buckle, I. G., Kelly, T. E., and Jones, L. R., AASHTO seismic isolation design requirements for highway bridges, *J. Struct. Eng. ASCE,* 118(1), 284–304, 1992.

39. Mayes, R. L., Jones, D. M., Knight, R. P., Choudhury, D., and Crooks, R. S., Seismically isolated bridges come of age, *Proc., 4th Intl. Conf. on Short and Medium Span Bridges,* Halifax, Nova Scotia, 1994, 1095–1106.

40. Nakashima, M., Strain-hardening behavior of shear panels made of low-yield steel. I: Test, *J. Struct. Eng. ASCE,* 121(12), 1742–1749, 1995.

41. Nanjo, A., Horie, Y., Okashiro, S., and Imoto, I., Experimental study on the ductility of steel bridge piers, *Proc. 5th International Colloquium on Stability and Ductility of Steel Structures — SDSS '97,* Vol. 1, Nagoya, Japan, 1997, 229–236.

42. NEHRP, Recommended Provisions for the Development of Seismic Regulations for New Buildings, Federal Emergency Management Agency, Washington, D.C., 1998.

43. Newmark, N. M. and Hall, W. J., *Earthquake Spectra and Design,* EERI, 1982.

44. Nishikawa, K., Yamamoto, S., Natori, T., Terao, K., Yasunami, H., and Terada, M., Retrofitting for seismic upgrading of steel bridge columns, *Eng. Struct.,* 20(4–6), 540–551, 1998.

45. Nishimura, N., Hwang, W. S., and Fukumoto, Y., Experimental investigation on hysteretic behavior of thin-walled box beam-to-column connections, in *Stability and Ductility of Steel Structures under Cyclic Loading,* Fukomoto, Y. and G. Lee, Eds., CRC, Boca Raton, FL, 163–174, 1992 .

46. Plumier, A., The dogbone: back to the future, *Eng. J., AISC,* 34(2), 61–67, 1997.

47. Popov, E. P. and Black, W., Steel struts under severe cyclic loading, *J. Struct. Div. ASCE,* 90(ST2), 223–256, 1981.

48. Popov, E. P. and Tsai, K.-C., Performance of large seismic steel moment connections under cyclic loads, *Eng. J. AISC,* 26(2), 51–60, 1989.

49. Priestley, M. J. N., Seible, F., and Chai, Y. H., Seismic retrofit of bridge columns using steel jackets, *Proc.* 10th World Conf. on Earthquake Eng., Vol. 9, Madrid, 5285–5290, 1992.

50. Roberts, J. E., Sharing California's seismic lessons, *Modern Steel Constr.*, AISC, 32(7), 32–37, 1992.

51. SAC, Interim Guidelines Advisory No. 1, Supplement to FEMA 267, Report No. FEMA 267A/SAC-96-03, SAC Joint Venture, Sacramento, CA, 1997.

52. SAC, Interim Guidelines: Evaluation, Repair, Modification, and Design of Welded Steel Moment Frame Structures, Report FEMA 267/SAC-95-02, SAC Joint Venture, Sacramento, CA, 1995.

53. SAC, Technical Report: Experimental Investigations of Beam-Column Sub-assemblages, Parts 1 and 2, Report No. SAC-96-01, SAC Joint Venture, Sacramento, CA, 1996.

54. SAC, Interim Guidelines Advisory No. 1, Supplement to FEMA 267, Report No. FEMA 267A/SAC-96-03, SAC Joint Venture, Sacramento, CA, 1997.

55. Sarraf, M. and Bruneau, M., Ductile seismic retrofit of steel deck-truss bridges. II: design applications, *J. Struct. Eng. ASCE,* 124 (11), 1263–1271,1998.

56. Sarraf, M. and Bruneau, M., Ductile seismic retrofit of steel deck-truss bridges. II: strategy and modeling, *J. Struct. Eng., ASCE,* 124 (11), 1253–1262, 1998 .

57. SEAOC, *Recommended Lateral Force Requirements and Commentary*, Seismology Committee, Structural Engineers Association of California, Sacramento, 1996.

58. Shirolé, A. M. and Malik, A. H., Seismic retrofitting of bridges in New York State," *Proc. Symposium on Practical Solutions for Bridge Strengthening and Rehabilitation,* Iowa State University, Ames, 123–131, 1993.

59. SSPC, *Statistical Analysis of Tensile Data for Wide Flange Structural Shapes*, Structural Shapes Producers Council, Washington, D.C., 1994.

60. Tide, R. H. R., Stability of weld metal subjected to cyclic static and seismic loading, *Eng. Struct.*, 20(4–6), 562–569, 1998.

61. Tsai, K. C., Chen, H. W., Hong, C. P., and Su, Y. F., Design of steel triangular plate energy absorbers for seismic-resistant construction," *Earthquake Spectra*, 9(3), 505–528, 1993.

62. Tsai, K. C. and Popov, E. P., Performance of large seismic steel moment connections under cyclic loads, *Eng. J. AISC,* 26(2), 51–60, 1989.

63. Tsai, K. C., Yang, Y. F., and Lin, J. L., Seismic eccentrically braced frames, *Int. J. Struct. Design Tall Buildings*, 2(1), 53–74, 1993.

64. Uang, C.-M., "Establishing R (or R_w) and C_d factors for building seismic provisions, *J. Struct. Eng.*, *ASCE,* 117(1), 19–28, 1991.

65. Usami, T. and Fukumoto, Y., Local and overall buckling tests of compression members and an analysis based on the effective width concept, *Proc. JSCE,* 326, 41–50, 1982. [in Japanese].

66. Usami, T., Mizutani, S., Aoki, T., and Itoh, Y., Steel and concrete-filled steel compression members under cyclic loading, in *Stability and Ductility of Steel Structures under Cyclic Loading*, Fukomoto, Y. and G. Lee, Eds., CRC, Boca Raton, 123–138, 1992.

67. Vincent, J., Seismic retrofit of the Richmond–San Rafael Bridge, *Proc. 2nd U.S. Seminar on Seismic Design, Evaluation and Retrofit of Steel Bridges,* San Francisco, 215–232, 1996.

68. Watanabe, E., Sugiura, K., Maikawa, Y., Tomita, M., and Nishibayashi, M., Pseudo-dynamic test on steel bridge piers and seismic damage assessment, *Proc. 5th East Asia-Pacific Conference on Structural Engineering and Construction,* Queensland, Australia, 1995.

69. Watanabe, E., Sugiura, K., Mori, T., and Suzuki, I., Modeling of hysteretic behavior of thin-walled box members, in *Stability and Ductility of Steel Structures under Cyclic Loading*, Fukomoto, Y. and G. Lee, Eds., CRC Press, Boca Raton, FL, 225–236, 1992.

70. Watanabe, E., Usami, T., and Kasegawa, A., Strength and design of steel stiffened plates — a literature review of Japanese contributions, in *Inelastic Instability of Steel Structures and Structural Elements*, Y. Fujita and T. V. Galambos, Ed., U.S.–Japan Seminar, Tokyo, 1981.

71. Yura, J. A., Galambos, T. V., and Ravindra, M. K., The bending resistance of steel beams, *J. Struct. Div. ASCE,* 104(ST9), 1355–1370, 1978.
72. Zahrai, S. M. and Bruneau, M., Impact of diaphragms on seismic response of straight slab-on-girder steel bridges, *J. Struct. Eng. ASCE,* 124(8), 938–947, 1998.
73. Zahrai, S. M. and Bruneau, M, Seismic Retrofit of Steel Slab-on-Girder Bridges Using Ductile End-Diaphragms, Report No. OCEERC 98-20, Ottawa Carleton Earthquake Engineering Research Center, University of Ottawa, Ottawa, Ontario, Canada, 1998.
74. Zekioglu, A., Mozaffarian, H., Chang, K. L., Uang, C.-M., and Noel, S., Designing after Northridge, *Modern Steel Constr. AISC,* 37(3), 36–42, 1997.